UC-413

LBL-28148

Lawrence Berkeley Laboratory

UNIVERSITY OF CALIFORNIA

To be published as a chapter in **Quark Gluon Plasma**, World Scientific Advanced Series in "Directions in High Energy Physics," R. Hwa, Ed., Singapore, Republic of Singapore

Non-Equilibrium Aspects of Ultrarelativistic Nuclear Collisions

M. Gyulassy

December 1989

For Reference

Not to be taken from this room

NUCLEAR SCIENCE DIVISION

LBL-28148
Copy 1
Bldg. 50 Library.

Prepared for the U.S. Department of Energy under Contract Number DE-AC03-76SF00098.

DISCLAIMER

This document was prepared as an account of work sponsored by the United States Government. While this document is believed to contain correct information, neither the United States Government nor any agency thereof, nor the Regents of the University of California, nor any of their employees, makes any warranty, express or implied, or assumes any legal responsibility for the accuracy, completeness, or usefulness of any information, apparatus, product, or process disclosed, or represents that its use would not infringe privately owned rights. Reference herein to any specific commercial product, process, or service by its trade name, trademark, manufacturer, or otherwise, does not necessarily constitute or imply its endorsement, recommendation, or favoring by the United States Government or any agency thereof, or the Regents of the University of California. The views and opinions of authors expressed herein do not necessarily state or reflect those of the United States Government or any agency thereof or the Regents of the University of California.

LBL-28148

Non-Equilibrium Aspects of Ultrarelativistic Nuclear Collisions [1]

Miklos Gyulassy[2]

Nuclear Science Division
Lawrence Berkeley Laboratory
Berkeley, CA 94720 USA

December 4, 1989

Abstract:
This review covers the following topics:

Dedication and Introduction 1
Outline 4
1. Tarnsport Models of A+A 5
1.1 Bevalac Lessons 5
1.2 Dissipation in Quark Gluon Plasmas 9
1.3 Toward QGP Transport Theory 11
1.4 Vacuum Dynamics 16
2. String Model Phenomenology from pp to AA
2.1 String Excitation 19
2.2 String Fragmentation 23
2.3 Color Ropes 27
2.4 From pp to pA to AA 28
3. Space-Time Aspects of Hadronization
3.1 Formation Zone in the Lund Model 33
3.2 Evolution of the Energy Density 35
3.3 Testing Phase Space Dynamics in eA 36
3.4 Pion Interferometric Tests of Transport Models 39
Concluding Remarks 43

[1] To appear in "Quark-Gluon Plasma", World Scientific Advanced Series in "Directions in High Energy Physics", edited by R. Hwa.

[2] Work supported by the U.S. Department of Energy under Contract DE-AC03-76SF00098

Non-Equilibrium Aspects of Ultrarelativistic Nuclear Collisions

Miklos Gyulassy[1]

Nuclear Science Division
Lawrence Berkeley Laboratory
Berkeley, CA 94720 USA

Dedication:

This report is based on a series of lectures that were to be given in a CCAST workshop in Beijing, China June 1-13, 1989. However, the tragic events that led to the crushing of the pro-democracy movement at that time of course terminated that workshop as well. I dedicate these lectures to my Chinese colleagues in solidarity with their aspirations, in memory of the innocent victims, and with the hope that the freedom and democracy will prevail eventually in China. The transition from totalitarianism to democracy has suffered a temporary setback, but the recent events in Eastern Europe and USSR testify that such transitions do exist in nature!

Introduction:

These lectures discuss aspects of an (analogous) confinement-deconfinement transition toward asymptotic freedom in the context of Quantum-Chromodynamics (QCD) and recent experimental attempts to observe that transition in high energy nuclear collisions. Because the signatures of equilibrated QGP are discussed by others in this review volume, I concentrate on non-equilibrium phenomena.

The primary motivation for studying high energy nuclear collisions is that they provide the only known way to probe the thermodynamic properties of ultra-dense hadronic matter directly in the laboratory [1]-[9]. The only other indirect means is to try to infer those from very limited cosmological and astrophysical data on the primordial nuclear synthesis abundances and neutron star characteristics. This has led to new experimental heavy ion program at CERN and BNL to study nuclear collisions at energies $E_{lab} = 10 - 200$ AGeV (GeV per incident projectile nucleon). The driving forces behind the present intense experimental effort are

1. the fundamental prediction of QCD that the thermodynamic properties of hadronic matter are expected to change dramatically when the energy density is only an order of magnitude beyond that found in ground state nuclei ($\epsilon_0 = 0.15$ GeV/Fm^3),

2. transport theory calculations indicating that energy densities up to $2 -$

[1]Work supported by the U.S. Department of Energy under Contract DE-AC03-76SF00098

20 GeV/Fm^3 could be reached in energy nuclear collisions over a space-time volume, $R^4 \gg 1$ fm^4, much larger than the characteristic confinement scale of QCD.

3. and the proven feasibility of accelerating nuclei to the required energies and of constructing experimental devices capable of measuring detailed properties of complex high multiplicity reactions.

In high energy nuclear reactions so many ($\sim$ thousands) of strongly interacting particles are produced that there is a possibility that a thermodynamic treatment may apply and that microscopic transport details may neglected. Even if approximate local thermal and chemical equilibrium is reached only for a few 10^{-23} seconds, then classical hydrodynamics could provide a direct link between the final observables such as the transverse momentum distribution, particle abundance ratios, fluctuations, etc. and the equation of state (pressure and entropy) of ultra dense matter.

Interest in that equation of state is due mainly to the predictions based on QCD lattice calculations that there exists a strong first order phase transition between the confined, chirally broken phase of QCD matter, referred to as hadronic or nuclear matter at low energy densities, $\epsilon \lesssim \epsilon_H \approx 0.5$ GeV/Fm^3, and a new deconfined, chirally symmetric phase of QCD matter, referred to as the quark gluon plasma (QGP) at high energy densities, $\epsilon \gtrsim \epsilon_Q \approx 2$ GeV/Fm^3. Such a phase transition is also predicted to lead to a number of interesting phenomena that could be looked for experimentally (see recent Quark Matter Proceedings and references therein).

Much excitement has been generated because of the data emerging from the first two years of experiments. A number of new phenomena were discovered to depend strongly on the nuclear atomic number, A. The NA38 collaboration found a factor of two suppression of J/Ψ in central $O+U$ at 200 AGeV. The E802 collaboration found a factor of four enhancement K^+/π^+ in central Si+Au collisions at 15 AGeV, and NA35 found indications for a factor of two enhancement of Λ production at 200 AGeV. Pion interferometry analysis of NA35 revealed evidence for an anomalously large pion decoupling volume. NA34 and WA80 revealed clearly the significant A dependence of the transverse energy and multiplicity distributions. The transverse momentum distributions were found to have an enhanced small $p_\perp$ component. Evidence for intermittent enhanced rapidity density fluctuations were also reported.

These results were especially remarkable because the the available nuclear beams were limited to very light ions O^{16} through S^{32}. The study of truly heavy nuclear collsions, e.g., $Au + Au$, will commence only after 1992, and the study of ultra-relativistic nuclear collisions with the heaviest nuclei and center of mass energies up to 100 AGeV will be possible only when the Relativistic Heavy Ion Collider (RHIC) at BNL is completed around 1996-7.

The important task in the next several years theoretically is to establish a quantitative understanding of the physics behind the strong A dependent phenomena observed so far and to develop a comprehensive transport theory for ultra-relativistic nuclear collisions. Are we seeing evidence already of the quark gluon phase transition or is that A dependence reflecting complex pre-equilibrium phenomena? The obvious complication that must be dealt with is that nuclei are finite and that the infinite volume thermodynamic limit may only be approached approximately. Corrections to ideal hydrodymics reflecting imperfect local equilibration may be substantial- especially for the light nuclear reactions studied up to now, where the typical hadronic mean free path $\lambda \sim 2$ fm is comparable to the nuclear radius. For such reactions we may even expect the dominance of non-equilibrium hadronic transport phenomena. It is also important investigate to what extent simple extrapolations of know hadron-hadron and hadron-nuclear reactions may provide a qualitative and even semi-quantitative explanation for many features of the data. In particular, is the strong A dependence observed in nuclear collisions simply an amplification of weaker A dependences observed in hadron-nucleus reactions or are there new nonlinearities?

I believe that the present data are teaching us about nonequilibrium hadronic phenomena. The main reason is that those data extrapolate smoothly from data on p+A, where similar though less dramatic phenomena are also found. In other words, there are no obvious threshold effects (as a function of multiplicity or transverse energy) that could signal the onset of plasma formation. Another point that I will discuss in section 3.2 is that there may be a good reason why plasma formation is not yet observed- namely, that the energy density in the present light ion reactions may be below the deconfinement threshold for most of the reaction time.

With regard to the first point, I note that the increase of the average transverse momentum of J/ψ's produced in $O+U$ as a function of transverse energy can be understood quantitatively by extrapolating the observed increase found in p+A relative to p+p (see S. Gavin p.447c [8]). Furthermore, the overall suppression can also be understood if new $\psi + meson \rightarrow D\bar{D} + X$ dissassociation processes in the dense comoving mesonic medium are taken into account. Other phenomena such as the enhanced Λ and K^0 production and an extra low $p_\perp$ component relative to that found in p+p are nearly identical to that seen in p+A reactions (see e.g. J. Harris, p.133c [8]). The large decoupling volume observed via pion interferometry can be understood when the nuclear geometry is folded together with effects due to long lived resonances (see S. Padula, p.489c [8]). The K^+/π^+ enhancement may be been accounted for by meson-nucleon and nucleon-nucleon associated $K^+\Lambda$ final state interactions (see H. Sorge et al Phys.Rev.Lett. 63 (1989) 1459). The point is that initial and final state hadronic processes lead to interesting new phenomena whether or not there is a plasma state produced. Indeed learning about the physics of dense hadronic matter is itself an important goal of heavy ion research.

The new physics associated with the onset of plasma formation at suffiently high multiplicities or transverse energies can only be identified if additional nonlinear behavior (beyond that expected from hadronic transport theory alone) is observed above some critical multiplicity or transverse energy. Up to now it apears that the observed nonlinearities can be understood without the additional plasma contribution.

The new data are very important even if such explanations are confirmed however because they provide the foundation for extrapolations to even heavier ion collisions and to even higher energies. Because the expected multiplicity and transverse energy systematics have been confirmed by the data, we now have a much greater degree of confidence in such extrapolations. Also the data constrain heretofore unknown elements in hadronic transport models such as the effective $\psi + meson \rightarrow D\bar{D} + X$ dissassociation cross sections mentioned above. Finally, direct evidence for final state interactions in light ion interactions is an essential prerequisite to the approximate local equilibration expected in collisions of heavier nuclei.

Outline:

Having introduced the context in which these lectures should be read, I outline next the contents of this report. These lectures are organized into three main sections: 1. Transport models for A+A, 2. String model phenomenology from pp to AA, and 3. Space-time aspects of hadronization. Section 1.1 begins by reviewing the progress made to extract the nuclear equation of state from nuclear collisions at low energies ($\sim$ 1 AGeV) from the Bevalac. It is emphasized that equilibrium properties can be extracted from heavy ion data only when the non-equilibrium tranport corrections are properly taken into account. In section 1.2 estimates for the shear and bulk viscocity transport coefficients in a quark gluon plasma indicate that non-equilibrium phenomena cannot be ignored in ultra-relativistic nuclear collisions either. Section 1.3 reviews some recent progress toward constructing a QCD transport theory. In section 1.4, I touch on the open and unsolved problems associated with transport phenomena of the non-perturbative vacuum itself! The Abelian-Higgs model of superconductivity illustrates why and how the dynamics of the vacuum condensates may be taken into account. Turning from the theoretical problems involved in contructing transport theories, section 2 concentrates on the phenomenology of string models for multiparticle production. Section 2.1 discusses how low transverse momentum gluon exchange can lead to color separation and string excitation. The mechanism of string fragmentation via $q\bar{q}$ pair production is reviewed in section 2.2. Possible novel non-equilibrium phenomena associated with multiple string fragmentation in terms of color ropes is discussed in section

2.3. Monte Carlo calculations of rapidity distributions and particle abundances in pp, pA, and AA are discussed in section 2.4. Finally in section 3, problem connected with space-time descriptions of multiparticle production are discussed. The formation zone in string models is reviewed in section 3.1 and the implications of this space-time picture on the evolution of the proper energy density in nuclear collsions is demonstrated in section 3.2. While considerable uncertainty remains about the basic space-time scales, it is shown that the light ion reactions studied up to now may reach energy densities above 1 GeV/Fm^3 for less than 1 fm/c- possibly explaning the success of conventional hadronic transport models in accounting for the bulk of the recent data. In section 3.3 turn to the problem of testing string dynamics in deep inelastic electron nucleus reactions. Finally in section 3.4, recent attempts to measure the space-time geometry of nuclear collisions via pion and kaon interferometry are discussed.

Of course these lecture illustrate only a few of the theoretical challenges facing current attempts to tackle non-equilibrium aspects of nuclear collisions. While incomplete, they hopefully help in identifying some of the important areas of current research.

1 Transport Models for A+A

1.1 BEVALAC Lessons

The importance of taking non-equilibrium transport phenomena into account in the collision of finite nuclei has been conclusively established in the energy range 0.1-2.0 AGeV. The study of nuclear collisions to learn about the properties of dense matter began 15 years ago[21], when the BEVALAC at LBL produced the first beams of light ions up to 2 AGeV. Present experiments are measuring detailed triple differential cross section of fragments produced in Au+Au collisions up to 1 AGeV. Hydrodynamics was recognized long ago here also as the most direct theoretical link between the sough after nuclear equation of state and the data. Calculations[22] soon suggested that nuclear collective flow phenomena were especially sensitive to the nuclear equation of state. However, as the data came to light, it soon became clear that finite mean free path effects could not be neglected. This led to the development of detailed Monte Carlo intra-nuclear cascade programs that could treat the correction due to non-equilibrium dynamics (see review [23]). Until it became possible to accelerate truly heavy ion beams with $A > 100$, most of the double differential data could in fact be well accounted for in terms of such cascade models.

The experimental breakthrough came in 1984, after a decade of light ion experiments, when conclusive evidence for collective nuclear flow was first found in Nb+Nb reactions[24] (see [25] for recent developments). The observed flow was

found to be much larger than predicted by cascade models but significantly smaller than expected on the basis of ideal hydrodynamics. These stimulated the development of much more elaborate non-equilibrium transport models such as Quantum Molecular Dynamics (QMD)[26] and Boltzmann-Uehling-Uhlenbeck (BUU)[27]. Those models take into account not only the stochastic two body scatterings but also the evolving mean nuclear potential, $U(\rho, p)$, that depends on the local nuclear density, $\rho(x)$, and on the momentum of the nucleon in the local rest frame. The generic form of such transport models is given by the Vlasov-Boltzmann equation:

$$(\partial/\partial t + p/m \cdot \nabla_x + (\nabla_p U \cdot \nabla_x - \nabla_x U \cdot \nabla_p))f(x,p,t) = C(f) \ , \tag{1}$$

where $f(x,p,t)$ is the phase space density of nucleons at time t, and the collision term is a nonlinear functional of f of the form

$$C(f) = \int dp_1 dp_1' dp' \{w(p'p_1' \to p, p_1) f' f_1'(1-f)(1-f_1) - (p \leftrightarrow p')(p_1 \leftrightarrow p_1')\} \ , \tag{2}$$

where $f = f(x,p,t), f' = f(x,p',t)$, etc. and $w = v_{rel} d\sigma/dpdp'$ is the differential collision cross section. The $(1-f)$ factors take into account Pauli blocking of the fermions. In practice (1) is solved by Monte Carlo simulation, following the trajectories of test particles in a self consistent mean field, U, and allowing stochastictic two body collisions when two particles pass each other at a distance closer than $\sqrt{(\sigma/\pi)}$.

The ideal (Euler) hydrodynamic equations follow from (1) by taking the first and second moments of that equation with respect to the momentum variable[28]. Those equations, $\partial_\mu T^{\mu\nu} = \partial_\mu j^\mu = 0$ simply express the conservation of energy momentum and baryon flux. Dynamical content to those equations is given only when the assumption of local equilibrium is made and the phase space density is assumed to have the form[28]

$$f_{eq}(x,p,t) \propto \exp(-(u(x)_\nu p^\nu - \mu(x))/T(x)) \ , \tag{3}$$

where $\mu(x)$, $T(x)$ are the chemical potential and temperature fields and $u^\nu(x)$ is the fluid four velocity field. The momentum tensor then has the form

$$T_{eq}^{\mu\nu} = (\epsilon + P)u^\mu u^\nu - P g^{\mu\nu} \ , \tag{4}$$

with $(\epsilon(T,\mu), P(T,\mu))$ denoting the thermodynamic proper energy density and pressure of the matter. This then is the formal connection between the equation of state of dense matter and nuclear collision dynamics.

Unfortunately, the thermal ansatz is never an exact solution of the transport equations for dynamical situations. While $C(f_{eq}) = 0$, the left hand side of the transport equation is proportial to the gradient of the thermodynamic quantities. Only if *global* equilibrium is achieved without gradients is (3) exact. Expanding

the exact phase space density around f_{eq}, as $f = f_{eq} + \delta f$, and approximating $C(f) \approx= -\delta f/\tau_c$ in terms of a characteristic relaxation time, τ_c, we obtain an estimate of $\delta f \propto \tau_c(p\partial_x + F\partial_p)f_{eq}$ to lowest order in the relaxation time. The existence of such a correction transforms the ideal Euler hydrodynamic equations into the Navier-Stokes equations ($\partial_\mu T^{\mu\nu} = 0$) with a modified momentum tensor

$$T^{\mu\nu} = T^{\mu\nu}_{eq} + \eta[\nabla u]^{\mu\nu} + \xi\nabla \cdot u\Delta^{\mu\nu} \quad , \tag{5}$$

where η, ξ are the shear and bulk viscosity coefficients and $\nabla^\mu = \Delta^{\mu\nu}\partial_\nu$ involves the local three frame projector $\Delta^{\mu\nu} = g^{\mu\nu} - u^\mu u^\nu$ ($[\nabla u]$ denotes the traceless gradient tensor). Heat conduction depends on the definition of the local rest frame. In the Landau definition it is the frame in which the local momentum flux vanishes, $T^{oi} = 0$. In that case the baryon current is given by $j^\nu = \rho u^\nu + \kappa\rho T/(\epsilon + P)\nabla^\nu(\mu(x)/T(x))$, involving the thermal conductivity coefficient, κ.

Kinetic theory leads to the familiar estimate

$$\eta = \frac{1}{3}\sum_i(\rho p\lambda)_i \quad , \tag{6}$$

where ρ_i is the proper density of particles of type i transporting an average momentum p_i over a momentum degradation mean free path λ_i. We can gauge the relative importance of transport corrections by estimating the effective pressure,

$$-T^{11} \sim \rho T(1 - O(\lambda/R)) \quad , \tag{7}$$

where we used $[\nabla u] \sim 1/R$ in terms of the characteristic radius of the interacting system. For nucleons, $\lambda \approx 2$ fm, while nuclear radii are typically $\sim 5fm$. Thus it was recognized long ago[29] that transport corrections are far from negligable and in fact finite nuclei should behave as very viscous fluids. Since corrections to Euler hydrodynamics are expected to be of order unity, the Navier-Stokes theory itself may not be adequate to decribe accurately the dynamics since it was derived under the assumption that transport corrections are small.

Detailed viscous hydrodynamics calculations of nuclear flow effects have confirmed the above expectations (see Stöcker in [25]). Experimentally, nuclear flow is studied by measuring the average in-reaction plane transverse momentum, $\langle p_x(y)\rangle$, of fragments as a function of the longitudinal rapidity of those fragments. Figure 1 shows the predicted transverse momenta based on Euler and Navier-Stokes equations. Indeed, viscous corrections are seen to reduce the flow momenta by a factor of two. However, when compared to actual measured values (see Fig.2), even the Navier -Stokes predictions exceed observations by a factor of two. Typically, experiment has revealed (see Fig.2) that $\langle p_x(y)\rangle \sim 50 - 100$ MeV/c even for the heaviest nuclei in contrast to the predicted 200 MeV/c with NS. This shows that the effective pressures are much smaller than they would be if local equilibrium were reached over a large volume of the nucleus.

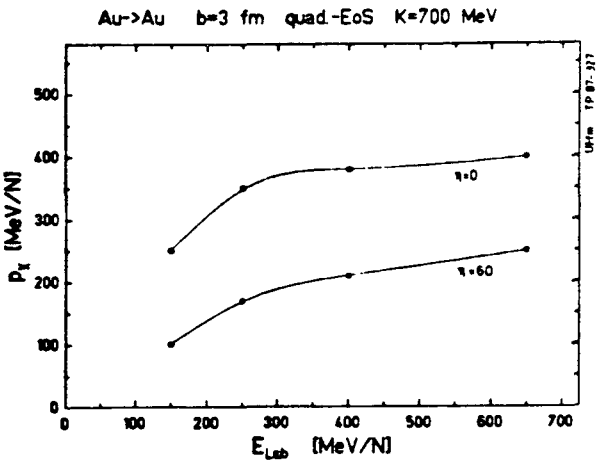

Figure 1: Mean transverse collective flow momenta as a function of energy from Euler ($\eta = 0$) and Navier-Stokes ($\eta = 60$ MeV/fm^2) (H. Stocker, et al)

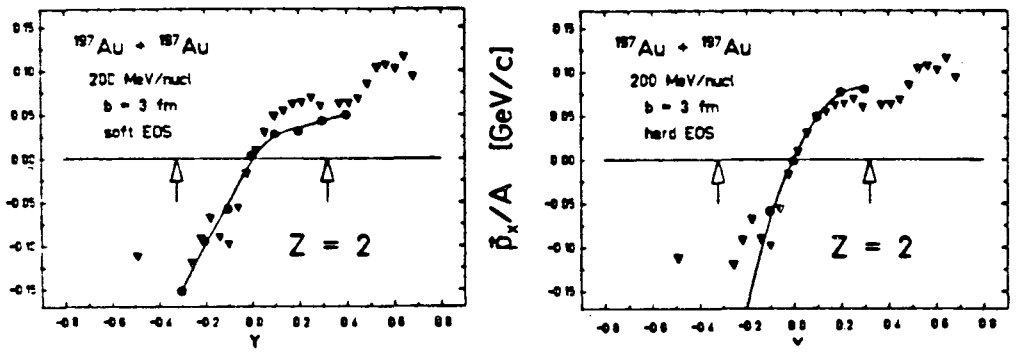

Figure 2: Data (K.H. Kampert, Munster PhD. thesis 1986) on transverse flow of $Z = 2$ fragments compared to QMD calculation (Peilert, et al) assuming a nuclear equation of state with incompressibility K=200 (soft) and 380 MeV (hard), respectively

Therefore, quantitative analysis of nuclear collision data requires the use of a microscopic transport theory. Figure 2 shows a recent analysis of collective flow based on the QMD model[26]. The sensitivity of flow phenomena to the equation of state is seen to be small ($\Delta p_x \sim 50$ MeV/c) as compared to the sensitivity (~ 200 MeV/c) of the results to the transport coefficients in Fig.1. This means that much higher statistics data and more refined transport calculations will be needed to converge on the nuclear equation of state. Impressive progress has been made recently[26,27] in refining nuclear transport theories, and measurements of triple differential cross sections are in progress. With the new GSI-SIS18 facility coming on-line this year and the completion of a new TPC at the BEVALAC it should be possible to obtain the required high precision data.

The BEVALAC lesson is clear. Detailed transport theories must be developed in order to cope with non-equilibrium phenomena dominating the reaction of even

the heaviest nuclei. Only from a careful, systematic study of detailed triple differential distributions as a function of nuclear size and beam energy can we expect to gain sufficient constraints on the many elements that go into such transport theories. Equilibrium properties of dense matter can be deduced from nuclear collsions only with a simultaneous determination of their transport properties.

1.2 Dissipation in QGP

In contrast to lower energies, where only nucleon and pion degrees of freedom are important, high energy nuclear collisions are complicated by the larger number of degrees of freedom involving the hadronic resonances such as the $\Delta, \omega, K^*, \cdots$ Also, while much is known about the interactions of pions and nucleons with each other, much remains to be learned about resonance dynamics. A rough estimate of the shear viscocity of a resonance gas can be obtained from (6) using a typical $\sigma \sim 10 - 20$ mb. This gives[30]

$$\eta_H \approx T/\sigma \approx 0.1 - 0.2(T(\mathrm{GeV})/0.2)\ \mathrm{GeV/fm}^2 \ . \tag{8}$$

To judge whether this is large or small we must estimate the gradients involved in high energy collisions. For longitudinal boost invariant boundary conditions, the Navier-Stokes equations reduce to[30]

$$d\epsilon/d\tau + (\epsilon + P)/\tau = (\frac{4}{3}\eta + \xi)/\tau^2 \ , \tag{9}$$

where τ is the proper time. Thus Navier-Stokes is valid only if the correction to the term proportional to the pressure is small, i.e. if $\eta \ll \tau P$, or $\sigma \gg T/(\tau P)$. If $P = c_H^2 \epsilon$, then in the absence of dissipation $P = P_0(\tau_0/\tau)^{1+c_H^2}$ and $T = T_0(\tau_0/\tau)^{c_H^2}$. Therefore, we must have $\sigma \gg T_0/(\tau_0 P_0) \equiv \sigma_c$. For $P_0 \sim 0.1$ GeV/Fm^3 in the hadronic phase at $T_0 \sim 0.2$ GeV and $\tau_0 \sim 1$ fm/c, $\sigma_c \sim 20mb$. Therefore, with our estimate of $\sigma \approx 20$ mb the hadronic expansion phase could be dominated by viscous effects just as it was found for the low energy nuclear collisions in the previous section.

Now condider the dynamics of the QGP phase. Here there is much more uncertainty because it is yet unclear what are the important dynamical degrees of freedom just above the phase transition temperature. Naive QCD perturbation calculation applied to an ideal Stefan Bolzmann gas of gluons and two flavors of quarks of density $n_q \approx n_g \approx 2T^2$ gives via (6)

$$\eta_Q \approx 2T^4(\lambda_q + \lambda_g) \ . \tag{10}$$

For one gluon exchange processes color factors lead to $\sigma(gg) = (9/4)\sigma(qg) = (9/4)^2\sigma(qq)$. Therefore the longest mean free paths are for quarks with $\lambda_q \approx 9/4\lambda_g$.

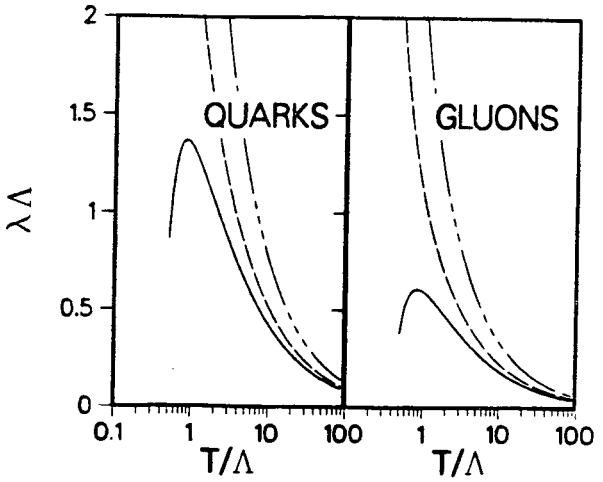

Figure 3: QCD perturbation estimates for the transport mean free paths of quarks and gluons as a function of temperature Upper and middle dashed curves correspond to $C = 30, 10$ respectively, while the solid curve include estimates for electric antiscreeing.

Quarks then dominate the transport coefficients. The perturbative transport cross section is given by[30]

$$\sigma_Q = -\int_{-s}^{0} dt \frac{\pi \alpha_T^2}{2} \left((t - m_E^2)^{-1} + (t - m_M^2)\right)^2 (4ts + t^2)/s^2 \ , \qquad (11)$$

where $\alpha_T \approx 1.2/\log(17T^2/\Lambda^2)$ is the effective coupling at high T and $m_E^2 \approx 4\pi\alpha_T T^2$ is the color electric screening mass and $m_M^2 = C\alpha_T^2 T^2$ is a nonperturbative color magnetic screening mass. Lattice QCD estimates suggest a $C \approx 30$. An important point made in ref.[31] is that dynamical screening in a plasma involving non zero frequency collisions are Landau damped, so that effectively all the Coulomb divergences are cut off at $\|t\| < m_E^2$. Numerically, for $\Lambda = 0.2$ GeV and $T = \Lambda$, $\alpha_T \sim 0.4$ and $m_E \approx m_M \approx 0.5$ GeV with $C = 30$ in the above formulas. Therefore inclusion of dynamical screeing does not change qualitatively the results in Fig.3. At low T nonperturbative antiscreening effects could cause m_E to decrease with T as $m_E^2(1 - \sqrt{\alpha_T})$. The transport cross section are unfortunately rather sensitive to the screening masses and the usual logrithmic approximation, $\sigma_\eta \propto \alpha_T^2/T^2 \log(T/m_E)$ is only accurate at extremely large $T \gg \Lambda$. Shown in Fig.3 are some numerical estimates of the transport mean free paths. Notice how painfully slowly do the mean free paths decrease with T. In the region of interest, $T \sim \Lambda$ there is obviously greatest uncertainty since α_T is no longer small. What Fig. 3 shows however is that large nonperturbative effects are needed to bring $\lambda_q + \lambda_g$ down to about $2\Lambda^{-1} \approx 2$ fm. At that point we would thus estimate $\eta_Q \gtrsim 4T^3$. To check whether the plasma evolution is viscous or not we compare the pressure, $P \approx 4T^4 \sim 0.8$ GeV/Fm^3 to the dissipative term $\eta/\tau \gtrsim 4T^3/\tau$. For $\tau \sim 1$ fm, we again see that the dissipative terms are of the same order as the pressure term. Therefore, this excercise leads us to expect that the entire expansion process would be highly dissipative.

There is yet another transport effect that needs to considered if there is a strong first order phase transition between the QGP and hadronic phases. That is the effect of bulk viscocity, ξ. As the system passes trough the mixed phase, the pressure remains constant, p_c, but the fraction of matter in the QGP phase decreases linearly as $\epsilon(\tau)$ decreases $\sim 1/\tau$ due to the rapid longitudinal expansion. However, their exists another characteristic relaxation time, τ_c, for the conversion rate between the two phases. This is a dynamical property of the phase transition itself and corresponds to a kind of nucleation time. Probably like all other scales in QCD, $\tau_c \sim 1$ fm. Given such a finite relaxation time, it is straightforward to show[30] that its effect is to reduce the pressure by an amount

$$p = p_c - \xi/\tau \ , \tag{12}$$

where the bulk viscocity coefficient is $\xi \approx c_p^2(\epsilon + p_c)\tau_c \sim p_c\tau_c$. Thus the transition through the mixed phase may also be highly dissipative.

We conclude that there is no a priori reason to expect ideal Euler hydrodynamics to provide an accurate account for the evolution of ultra-relativistic nuclear collisions, and just as in the BEVALAC case it is likely that a full transport calculation will be required.

1.3 Toward QGP Transport Theory

In formulating a QCD transport theory a primary constraint is to insure gauge invariance. We review here some preliminary work[32,33,34] on this problem. Under a general non-Abelian gauge transformation, $G(x) = \exp(i\theta_a(x)t_a)$, the fields, $\psi(x)$ and $A_\mu(x)$, in the fundamental and adjoint representations transform as

$$\psi(x) \to G(x)\psi(x) \ , \ A_\mu(x) \to G(x)A_\mu(x)G^\dagger(x) + G(x)\partial_\mu G^\dagger(x)/(ig) \ . \tag{13}$$

Thus, the covariant derivative and field tensor transform covariantly, i.e., $D_\mu(x) \to G(x)D_\mu(x)G^\dagger(x)$. Transport theory focuses on the Wigner density operator[28] corresponding to the classical phase space density. A natural first guess for that operator is

$$\hat{W}_{\alpha\beta}(x,p) = \hat{\bar{\psi}}_\beta \delta^4(p - \hat{p})\hat{\psi}_\alpha(x), \tag{14}$$

where $\hat{p}$ is the momentum operator since then $f(x,p) \equiv \langle Tr\hat{W}(x,p)\rangle$ would have the interpretation of a scalar density of quanta carrying momenta p. However, (14) is not satisfactory for gauge theories because $f(x,p)$ would not be gauge invariant. The problem is that ordinary derivatives do not commute with $G(x)$. This problem can be overcome by recalling that in classical electrodynamics the kinetic momentum is given by $\pi^\mu = p^\mu - eA^\mu$, where p^μ is the *canonical* momentum conjugate to the coordinate x^μ. Thus it is the the covariant derivative rather than

the ordinary derivative that represents the *kinetic* as opposed to the *canonical* momentum. We are thus led to define the gauge covariant Wigner operator as

$$\hat{W}(x,p) = \bar{\psi}(x)\,\delta^4(p-\hat{\pi}(x))\;\psi(x) = \int \frac{d^4y}{(2\pi)^4} e^{-ip\cdot y}\;\bar{\psi}(x) e^{\frac{1}{2}y\cdot D^\dagger(x)} \otimes e^{-\frac{1}{2}y\cdot D(x)}\psi(x)\;. \tag{15}$$

The symbol $\otimes$ indicates that $\hat{W}$ is a 4×4 matrix in spinor indices and a $N\times N$ matrix in color indices. Because $\hat{\pi}_\mu$ transforms covariantly, not only have we achieved gauge covariance but also $\langle Tr\hat{W}(x,p)\rangle$ has the desired interpretation of being the gaude invariant, Lorentz scalar density of particles at x with kinetic momentum p.

The equation of motion for $\hat{W}$ can be derived from the Dirac equation[34], with the result

$$\left(\gamma^\mu p_\mu - m + \tfrac{1}{2}i\hbar\gamma^\mu \mathcal{D}_\mu(x)\right)\hat{W}(x,p)$$

$$= \tfrac{1}{4}\hbar g\gamma_\mu\left(\{Q_1(\tfrac{1}{2}\hbar\Delta)\,F_{\mu\nu}(x), \partial^p_\nu W(x,p)\} + \;[Q_2(\tfrac{1}{2}\hbar\Delta)\,F_{\mu\nu}(x), \partial^p_\nu W(x,p)]\right)\;, \tag{16}$$

where

$$\begin{aligned} Q_1(x) &= i\frac{\sin x}{x} + \frac{\sin x - x\cos x}{x^2}\;, \\ Q_2(x) &= i\frac{x\sin x + \cos x - 1}{x^2} + \frac{1-\cos x}{x}\;. \end{aligned} \tag{17}$$

and the *triangle operator*, Δ, is given in this case by

$$\Delta = \partial_p\cdot\mathcal{D} = \partial_p\cdot\partial_x + \frac{1}{\hbar}ig\partial_p\cdot[A(x),\;\;]\;, \tag{18}$$

We emphasize that $\mathcal{D}(x)$ on the right hand side only acts on $F_{\nu\mu}$. Because $\mathcal{D}_\mu$, $F_{\mu\nu}$, Δ and $\hat{W}(x,p)$ transform covariantly under a gauge transformation, eq.(16) is a *gauge covariant operator equation* of motion.

Equation (16) is completely equivalent to the original Dirac's equation for the Heisenberg field $\hat{\psi}$. However, it is in a form that allows us to extract the quantum transport equation. In fact contains two equations. One is the generalized quantum transport equation. The second is a generalized mass shell constraint equation that arises on account of the Heisenberg uncertainty principle.

The physical content of (16) is especially clear in the Abelian limit when in addition $F_{\mu\nu}$ is replaced as the self-consistent c-number field. In the Hartree approximation in which $F_{\mu\nu}$ is approximated by the mean (c-number) field $\bar{F}_{\mu\nu}$ satisfying Maxwell's equations

$$\partial_\mu\bar{F}^{\mu\nu}(x) = \langle J^\mu(x)\rangle = e\,tr\int d^4p\,\gamma^\mu\,W^H(x,p)\;. \tag{19}$$

The trace is over spinor indices of $W^H(x,p) = \langle \hat{W}(x,p) \rangle$ corresponding to the ensemble average of the Wigner operator in the Hartree approximation. In this case the *triangle operator* is simply the mixed derivative

$$\Delta \equiv \partial^p \cdot \partial_x \ . \tag{20}$$

Notice that the triangle operator has the dimension of inverse action so that in units where $\hbar \neq 1$ it always appears multiplied by $\hbar$. Therefore, a power series expansion of the Bessel functions coincides with an expansion in terms of the ratio of $\hbar$ to a characteristic angular momentum, L, of the plasma. That characteristic angular momentum measures the product of the space-time scale, ΔR_F, over which the field tensor, $\bar{F}^{\mu\nu}(x)$, varies appreciably and the momentum scale, ΔP_W, over which the Wigner function varies appreciably. Therefore, a necessary condition for the validity of a power series expansion of the Bessel functions is that the mean field is slowly varying in the sense

$$\hbar \ll \Delta R_F \Delta P_W \ . \tag{21}$$

In the Abelian case the linear equation (16) can be written in the following suggestive form:

$$(\gamma \cdot K - m)\, W^H(x,p) = 0 \ , \tag{22}$$

in terms of the operator $K^\mu \equiv \Pi^\mu + \frac{1}{2} i\hbar \nabla^\mu$, where

$$\nabla^\mu \equiv \partial^\mu_x - e j_0(\tfrac{1}{2}\hbar\Delta)\, \bar{F}^{\mu\nu}\, \partial^p_\nu \ , \tag{23}$$

$$\Pi^\mu \equiv p^\mu - \tfrac{1}{2}\hbar e j_1(\tfrac{1}{2}\hbar\Delta)\, \bar{F}^{\mu\nu}\, \partial^p_\nu \ , \tag{24}$$

and where $j_i(x)$ are conventional spherical Bessel functions. We have reinstated $\hbar$ explicitly to show clearly the quantum character of this equation. To lowest order in $\hbar$ these operators reduce to $\nabla^\mu = \partial^\mu_x - e\bar{F}^{\mu\nu}\partial^p_\nu$ and $\Pi^\mu = p^\mu$. The constraint and transport equations can be extracted by first multiplying (22) by $(\gamma \cdot K + m)$ and adding and subtracting the adjoint of this equation. We thus recover the familiar Vlasov equation

$$\Pi^\mu \nabla_\mu\, W^H(x,p) = 0 \ , \ (\Pi^2 - m^2) W^H(x,p) = 0 \ , \tag{25}$$

where the second equation is just the mass-shell equation.

We turn next to the non Abelian features of (16). There is a very important difference between the triangle operator expansion in the Abelian and non-Abelian cases. The Abelian expansion is equivalent to the semiclassical expansion in powers of $\hbar$. In the non-Abelian case, there appears a commutator in (18) that is of *zeroth* order in $\hbar$!! We can still write the linear operator equation in the form (22).

However, the operators Π^μ and ∇^μ are now given by

$$\nabla^\mu \equiv \mathcal{D}^\mu_x \;-\; \tfrac{1}{2}g\{ImQ_1(\tfrac{1}{2}\hbar\Delta)\,F_{\mu\nu},\ \}\,\partial^p_\nu - \tfrac{1}{2}g[ImQ_2(\tfrac{1}{2}\hbar\Delta)\,F_{\mu\nu},\ ]$$

$$= \frac{1}{\hbar}ig[A^\mu(x),\ ] \;+\; \partial^\mu_x - \tfrac{1}{2}g\{F_{\mu\nu},\ \}\partial^p_\nu - \tfrac{1}{24}g^3\{[A^\alpha,[A^\beta,F_{\mu\nu}]],\ \}\partial^p_\nu\partial^p_\alpha\partial^p_\beta + \cdots\ ,$$

$$\Pi^\mu \equiv p^\mu \;-\; \tfrac{1}{4}\hbar g\left(\{ReQ_1(\tfrac{1}{2}\hbar\Delta)\,F_{\mu\nu},\ \} + [ReQ_2(\tfrac{1}{2}\hbar\Delta)\,F_{\mu\nu},\ ]\right)\partial^p_\nu\ . \qquad (26)$$

We see that something terrible has happened. The non-Abelian commutator has changed the leading order in $\hbar$ for the operator ∇^μ to be $O(1/\hbar)$, and there now arise an infinite number of commutators and anti-commutators to zeroth order in $\hbar$. Thus the simple classical limit we found in the Abelian case becomes hopelessly complicated in the non-Abelian case.

The only simple semiclassical limit of a non-Abelian theory is one where the *covariant* derivative of $F_{\mu\nu}$ is small. Only for covariantly slowly varying fields, in the sense that

$$\langle F\hat{W}\rangle \gg \langle \mathcal{D}F\ \partial_p\hat{W}\rangle\ , \qquad (27)$$

is it possible to carry out an expansion in powers of the Δ operator. In particular for covariant constant fields, the linear operator equation for $\hat{W}$ reduces to

$$\left(\ \gamma_\mu(p^\mu + \tfrac{1}{2}i\hbar(\mathcal{D}^\mu - \tfrac{1}{2}g\{F_{\mu\nu},\ \}\partial^p_\nu - \tfrac{1}{4}g[F_{\mu\nu},\ ]\partial^p_\nu) - m\ \right)\hat{W}(x,p) = 0\ . \qquad (28)$$

In the general case for strong or rapidly varying fields the full quantum equation, eq.(16), must be solved. This would be equivalent to solving the original field equations, i.e. hopeless at this time. Only under the rather restrictive conditions, (27), can we expect that the transport theory for quarks reduces to a simpler, more manageable form.

For covariant constant or slowly varying fields, the color structure of the above equation is particularly transparent. We consider essentially Abelian fields such that all components of $F_{\mu\nu}$ can be simultaneously diagonalized in the same gauge:

$$\langle F^{\mu\nu}(x)\rangle \equiv S(x)\vec{F}^{\mu\nu}\cdot\vec{h}S^{-1}(x)\ , \qquad (29)$$

where h_i the $N-1$ diagonal Gell-Mann matrices and $S(x)$ is a particular gauge transformation. We now make the bold model dependent *ansatz* that the ensemble of quarks is such that $\hat{W}$ is diagonal in the *same* gauge where $\langle F_{\mu\nu}(x)\rangle$ is diagonal. By assumption then we can express

$$\langle\hat{W}\rangle \equiv S(x)\left(\sum_{j=1}^{N-1} W^j h_j + W^0\mathbf{1}\right)S^{-1}(x)\ , \qquad (30)$$

in terms of N Wigner *functions* depending on (x,p). Equation (30) is a strong model assumption and we refer to it as the Abelian Dominance Approximation

[34]. There is no guaranty that such ensembles of quarks exist in nature or how well they approximate the conditions of the quark-gluon plasma formed in nuclear collisions. We proceed in the spirit of the MIT bag and string models and adopt this assumption for phenomenological purposes.

When (30) holds, it is most convenient to work in the $S(x)$ gauge, where

$$\langle \hat{W} \rangle_{ij} = (\vec{W} \cdot \vec{h} + W^0_{ij} \mathbf{1}) = \delta_{ij}(\vec{W} \cdot \vec{\epsilon}_j + W^0) \equiv \delta_{ij} f_j \ , \tag{31}$$

where the "charges" $\vec{\epsilon}_j$ are just the elementary weight vectors of SU(N).

The semiclassical transport equations for the $f_j(x,p)$ in this approximation are then found to be

$$(p \cdot \partial_x + g\vec{\epsilon}_j \cdot \vec{F}_{\mu\nu} p^\nu \partial^\mu_p)\ f_j(x,p) = -\tfrac{1}{4} i g \vec{\epsilon}_j \cdot \vec{F}_{\mu\nu} [\ \sigma^{\mu\nu}, f_j(x,p)\ ] + \tilde{C}_j(x,p) \quad , \tag{32}$$

where $\tilde{C}_j$ represents correlation terms of the form

$$\tilde{C}_j(x,p) = -\tfrac{1}{2} g p^\mu \partial^\nu_p \left(\langle \{ F_{\nu\mu}, \hat{W}(x,p) \} \rangle - 2 \langle F_{\nu\mu} \rangle \langle \hat{W}(x,p) \rangle \right)_j + \cdots \quad . \tag{33}$$

As usual, the collision terms are contained in such correlations.

Note that all the non-Abelian commutator terms dropped out for the model *ansatz* (30) and the transport theory for quarks has reduced to an effective multi-component Abelian plasma theory. The $f_i(x,p)$ just correspond to the phase space densities for quarks with "charge" $g\vec{\epsilon}_i$. Quarks then obey an effective Abelian Vlasov equation with the same in an effective Abelian field $e_i F^{\mu\nu}_{eff} = g\vec{\epsilon}_i \cdot \vec{F}^{\mu\nu}$. Therefore, the quark plasma dynamics is very simple and intuitive in this Abelian Dominance Approximation.

Transport of gluons can be considered along similar lines[34] in terms the gauge covariant gluon Wigner operator

$$\hat{\Gamma}_{\mu\nu}(x,p) \equiv \int \frac{d^4 y}{(2\pi)^4} e^{-ip\cdot y} [e^{\frac{1}{2} y \cdot \mathcal{D}(x)} F_\mu{}^\lambda(x)] \otimes [e^{-\frac{1}{2} y \cdot \mathcal{D}(x)} F_{\lambda\nu}(x)] \ , \tag{34}$$

$\hat{\Gamma}$ is closely related to the energy-momentum tensor of the field. In the Abelian Dominance Approximation, the equations of motion for the $N^2 - 1$ gluon densities reduce to a set of effective Abelian Vlasov equations, with $\vec{\epsilon}_i$ replaced by $\vec{\eta}_{ij} = \vec{\epsilon}_i - \vec{\epsilon}_j$ for the $N(N-1)$ "charged" gluon densities and 0 for the $N-1$ "neutral" ones.

The multicomponent plasma equations resulting in the Abelian Dominance Approximation have a number of interesting consequences. As reviewed in [36], they can be used to derive the same electric screening mass and plasmon oscillation frequencies as found in using diagrammatic QCD perturbation theory. Two stream instabilities in inter-streaming QGP have also been considered. Some of the outstanding open problems at present is how to include quantum pair production processes as source terms in the transport equations and how to include Debye screened effective collision terms (see recent review [35]). Phenomenological source terms have been considered for example in [37] and novel oscillations were predicted to occur in the expanding QGP at high energies that could have observable consequences.

1.4 Vacuum Dynamics

A critical problem at the heart of any attempt to formulate a QGP transport theory is the problem of confinement. All attempts to formulate transport theory have thusfar assumed that we can start with the perturbative vacuum and go from there. However, the problem is that nuclear collisions occur in the physical, highly nonperturbative vacuum that is responsible for confinement. If an ideal QGP were to be created, then at least in the interaction region, the non-perturbative fluctuations must be suppressed on a fast time scale. It is not known yet what are the most important vaccum fluctuations in QCD that give rise to confinement. One attractive idea[38] is that due to the very singular infrared properties of the color magnetic sector a condensate of non-perturbative color magnetic monopole pairs are created. In analogy with superconductivity, such a condensate of magnetic monopoles could produce a color electric Meissner effect which expels color electric fields from the vacuum. Deconfinement in this analogy would occur at a critical temperature when the condensate "evaporates" and the Meissner effect disappears. Of course, there exists a time scale (leading to bulk viscocity) associated with this quenching transition.

Consider the analog Abelian problem of the transport of magnetic monopoles and antimonopoles in a an infinite superconductor. At very low densities, magnetic fields will be squeezed into non-overlapping flux tubes binding monopole antimonopole pairs. This is the analog of the hadronic world. As the density of these flux tubes increases the average local magnetic field increases and at some critical density the magnetic fields become so large that the Cooper pairs dissolve and the Meissner effect disappears. The monopole pairs in that region will then be free to wander around without the confining flux tubes and will form a plasma with Debye screened magnetic interactions. The interesting problem from this point of view is to calculate the dynamics of a colliding group of flux tubes, and see if there is sufficient time for the Cooper pairs to react to allow the formation of such a plasma. If there is, then the next interesting question is to determine how the reformation of the condensate affects the final dynamics as the monopole pairs expand and reconfine themselves. This analog model involves then the transport dynamics of the underlying non-perturbative medium as well as of the monopoles.

There has been some progress recently toward numerical solutions of interacting vortices[39]. A dynamical model with the above properties is provided Abelian-Higgs model of Ref.[40]. The Lagrangian involves U(1) gauge theory coupled to a complex Higgs field, ϕ via

$$\mathcal{L} = -\frac{1}{4}F^2 + \frac{1}{2}(D\phi)^2 - V(\phi) - ej_{ex}A \ , \tag{35}$$

where $D = \partial + ieA$ is the covariant derivative and $V = -\frac{1}{2}\mu^2\phi^2 + \frac{c^2}{4}\phi^4$ is chosen to give the Higgs field a negative mass balanced by a quartic repulsive interaction.

It is convenient to write $\phi = \sigma \exp(i\chi)$. Consider finite vorticies generated by monopole-antimonopole pairs[41]. Taking $\chi = 0$ and the $\partial A = 0$ gauge, in the absence of external electric charges the static field equations simplify to[42]

$$\begin{aligned}(\nabla^2 - e^2\sigma^2)\vec{A} &= e\vec{j}_{ex} \ , \\ (\nabla^2 - e^2 A^2)\sigma &= \mu^2\sigma((\sigma/\sigma_0)^2 - 1) \ ,\end{aligned} \tag{36}$$

The vacuum state is thus given by $\vec{A} = 0$, but $\sigma = \sigma_0 = \mu/c$ is nonvanishing. A pair of monopoles located on the z-axis at points $z = \pm a$ can be represented by a finite solenoid with a current of the form

$$\vec{j}_{ex}(z,\rho) = g\hat{e}_\theta(\Theta(z+a) - \Theta(z-a))\partial_\rho\delta(\rho^2) \ , \tag{37}$$

where g is the monopole charge. We see that far from the source A must decrease exponentially on a scale $\lambda = 1/e\sigma_0 = c/e\mu$ called the London penetration length while the Higgs field returns to its vacuum value on a coherence scale, $\xi = 1/\mu$. In a type II superconductor the penetration length exceeds the coherence length, i.e. $c > e$. In variational calculations with this model to fit charmonium levels, the parameters found indicated that the effective penetration length was only $\lambda \sim 0.3$ fm. This is much smaller than the naive MIT Bag model estimates of $\lambda \approx 1.6$ fm, which results from the use of a much smaller Bag constant (~ 0.05 GeV/Fm^3) than found from QCD sum rules[9] (~ 0.5 GeV/Fm^3). Such thin vorticies could have important consequences for constructing transport theories for nuclear collisions. As we discuss in the next section, the success of independent multi-string models in describing data is difficult to understand when string densities $\sim 2/\text{fm}^2$ are expected except if the string radii were unusually small. The Abelian Higgs model may provide the necessary insight into the physics that controls such scales.

Equally importantly that model can be studied dynamically to see the interplay between the Higgs vacuum and the evolving gauge fields. In Fig. 4, numerical solution for the scattering of two right angle vorticies from ref.[39] is shown. This shows that dynamical calculations taking into account the vacuum properties may be possible eventually. This is only an analog toy model, but work on such models may help in formulating effective QCD transport models.

Another approach to study vacuum dynamics may involve the Friedberg-Lee Dielectric Model (FLDM) [43] with

$$\mathcal{L} = -\frac{1}{4}\kappa(\sigma)F^2 + \frac{1}{2}(\partial\sigma)^2 - V(\sigma) - ej_{ex}A \ , \tag{38}$$

where $\kappa(\sigma)$ is a dynamical dielectric function that depends in this case on a neutral scalar field σ with the property that $\kappa(\sigma_0) = 0$. Wilets and collaborators[44] showed that such a model could account well for hadron spectroscopy and emphasized its value in dynamical calculations. It leads naturally to MIT Bag model type flux tubes with finite surface thickness.

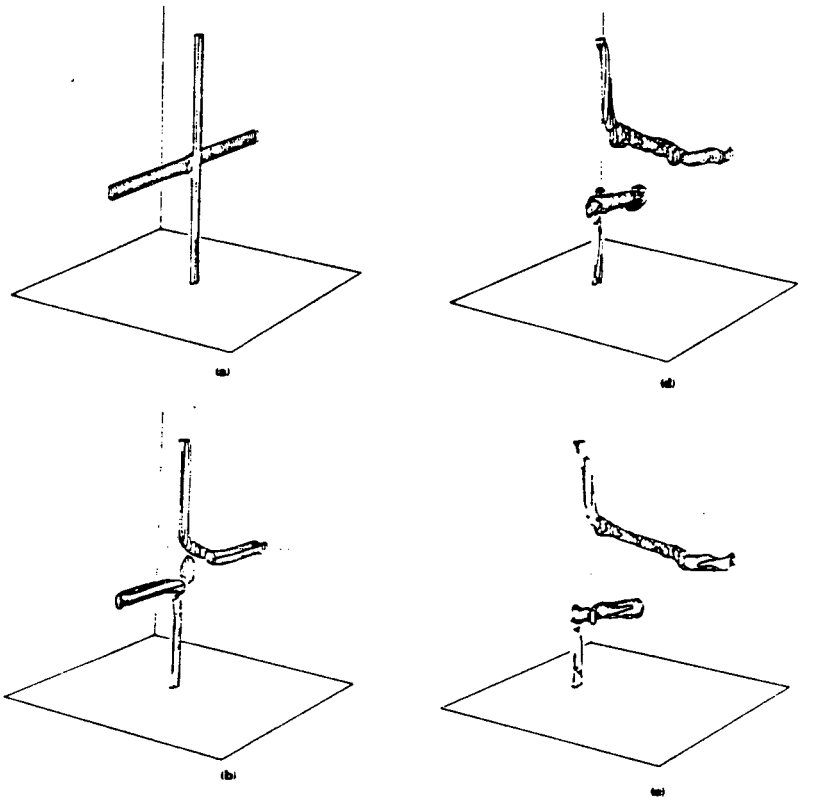

Figure 4: Scattering of vorticies at right angles in the Abelian-Higgs model (Matzner) leading to a "string" flip. Contours indicate regions where the Higgs field is reduced to 40% its vacuum value.

The above models are Abelian analog models of confinement. Dynamical models with non-Abelian effects could of course differ dramatically. One possibility studied recently is that large high amplitude oscillations of classical non-Abelian fields could exhibit chaotic as opposed to ordered plasmon like oscillations. It could be that the strong self coupling of the transient gluon fields in nuclear collisions could play an important role melting the vacuum and thermalizing the QGP. Such ideas also need further exploration.

2 String Model Phenomenology from pp to AA

2.1 String Exitation

While work is progressing on the construction of an effective QGP transport theory, it is necessary to turn to phenomenology to help assess the significance of the strong A dependence found for many observables in nuclear collisions. The color flux tube or string model phenomenology, developed extensively in refs.[10]-[20], has proven to be very useful in this connection. Since detailed fits of such models to AGS and SPS data are covered by other speakers, I focus here on the general theoretical perspective.

The basic mechanism of string formation in soft hadronic processes is assumed in many models to arise from the scattering of color charged partons. Differences between models arise by the choice of which partons interact and how the color indicies are connected at the end. We recall briefly how string excitation works in such models. Consider the scattering of two hadrons with initial light cone momenta

$$P_1 = (E_1^+, m^2/E_1^+, 0_\perp) \ , \ \ P_2 = (m^2/E_2^-, E_2^-, 0_\perp) \ , \tag{39}$$

such that $E_1^+ \gg m$ and $E_2^- \gg m$. Suppose that two participant partons with

$$k_1 \approx (x^+ E_1^+, 0, 0_\perp) \ , \ \ k_2 \approx (0, x^- E_2^-, 0_\perp) \tag{40}$$

scatter on-shell as a result of a small momentum transfer

$$q = (-q_+, q_-, q_\perp) \sim O(m) \ . \tag{41}$$

For scattering on-shell $q^\pm$ are constrained to be[10]

$$q_+ \approx q_\perp^2/(x^- E_2^-) \ , \ \ q_- \approx q_\perp^2/(x^+ E_1^+) \ . \tag{42}$$

This small momentum transfer leads on the other hand to a large rapidity gap between the participant and spectator partons with $\Delta y \sim \log 1/x^\pm$. Confinement then forces the color electric field between the separating participant and spectator

partons into two narrow flux tubes or strings. A string is characterized by the flavor quantum numbers and the sum of the four momenta of the end point partons. If no color is exchanged, as assumed in the LUND model FRITIOF[10], the two strings formed by the low $p_\perp$ elastic scattering of two $x^\pm \ll 1$ (wee) partons end up with momenta

$$\begin{aligned} P_1' &= P_1 + q \approx (E_1^+ - q^+, q^-, q_\perp) \\ P_2' &= P_2 - q \approx (q^+, E_2^- - q^-, q_\perp) \ . \end{aligned} \tag{43}$$

The invariant masses of the two strings can thus be rather large in the limit $x\pm \to 0$:

$$M_1^2 \approx q_\perp^2/x^+ \ , \ M_2^2 \approx q_\perp^2/x^- \ . \tag{44}$$

On the other hand, if color exchange occurs, as assumed in the DPM[11], the strings attached to the participant partons must be reconnected to the spectators of the opposite hadron. The four momenta of the two strings in this case are thus

$$\begin{aligned} P_1' &= P_1 - k_1 + k_2 - q \approx ((1-x^+)E_0^+, x^- E_0^-, q_\perp) \\ P_2' &= P_2 - k_2 + k_1 + q \approx (x^+ E_0^+, (1-x^-)E_0^-, -q_\perp) \ , \end{aligned} \tag{45}$$

with invariant masses

$$M_1^2 \approx x^-(1-x^+)s \ , \ M_2^2 \approx (1-x^-)x^+ s \ , \tag{46}$$

with $E_0^\pm = P_1^\pm + P_2^\pm$ and $s = E_0^+ E_0^-$.

The probability for a particular string excitation is thus fixed in both cases by the probability $p(x^+, x^-, q_\perp)$, that two partons with fractional light cone momenta, $x^\pm$, scatter on-shell with transverse momentum exchange, $q_\perp$. Unfortunately, p depends on the structure functions and parton-parton cross sections at a scale, $q_\perp \lesssim 1$ GeV/c, where perturbation theory breaks down and no reliable QCD predictions are possible. Therefore, p must be considered as a phenomenological function that is to be fixed by fitting multiparticle production data. In most cases, p is assumed to factorize as

$$p(x^+, x^-, q_\perp) = g(x^+, x_0^+) g(x^-, x_0^-) g_\perp(q_\perp) \ , \tag{47}$$

where $x_0^\pm$ are kinematic lower bounds that tend to zero at high energies. Given the "excitation" function, $g(x, x_0)$, and the transverse momentum distribution , $g_\perp(q_\perp)$, the string mass distribution is

$$dP/dM^2 = \int_{x_0^\pm}^{1-x_0^\pm} g(x^+, x_0^+) g(x^-, x_0^-) \int d^2 q_\perp g_\perp(q_\perp) \delta(M^2 - M^2(x^+, x^-, q_\perp) \ . \tag{48}$$

Three popular forms for the excitation function used in current models[10,11,18]:

$$g(x, x_0) = \begin{cases} x^{-1} \{\ln((1-x_0)/x_0)\}^{-1} & \text{LUND} \\ x^{-\beta} \{((1-x_0)^{1-\beta} - x_0^{1-\beta})/(1-\beta)\}^{-1} & \text{DPM} \\ \alpha(1-x_0-x)^{\alpha-1}\{1-2x_0\}^{-1} & \text{MCM} \end{cases} \ . \tag{49}$$

These functions are normalized such that

$$\int_{x_0}^{1-x_0} dx g(x, x_0) = 1 \ .$$

The choice of the finite energy cutoffs, $x_0^{\pm}$, is obviously not unique, but it is expected that at sufficiently high energies results will be insensitive to their exact values.

The LUND ansatz[10] is motivated by parton phenomenology, where it is assumed that only wee partons interact. The $1/x$ distribution provides a natural explanation via (48) for the observation that the mass distribution in single diffractive events is well approximated by dM/M and that the multiplicities and rapidity densities from the diffractive cluster are very similar to those in non-diffractive events with $s = M^2$. The similarity between single diffractive and non-diffractive event structures at the same cm energy follows from that law as well since on the average the two excited strings span the rapidity gap without overlapping. Finally the observed asymmetry of the diffractive rapidity density around its cm rapidity follows because $q - (qq)$ strings tend to fragment in to meson on the q end and a baryon on the qq end. By momentum conservation the meson will have about 1 unit larger rapidity than the baryon.

It is important to note that for large mass strings, Lund strings are also allowed to carry transverse vibrations representing gluons[10]. Those vibrations are introduced to account for the high multiplicity tails in pp collisions. However, we restrict all further consideration to simple strings without gluon kinks since at the present energies they are adequate for our applications.

The Dual Parton Model ansatz is motivated by Regge phenomenology and the small x behavior of parton distributions[11,14]. It is assumed that instead of the wee partons, the valance quarks are most effective in color exchange. The valance quark distribution at small x is of the form $1/\sqrt{x}$ corresponding to $\beta = 1/2$ in (49). However, in subsequent parton interactions it is assumed that only wee partons participate, corresponding to $\beta = 1$ in (49). Thus, the excitation laws in LUND and DPM differ only for the first string excitation. We also note that even though the invariant mass formulas for the two models are so different, the mass distribution (48) with $g \sim 1/x$ is $1/M$ for both mass formulas in the range $m \ll M \ll \sqrt{s}$. In recent refinements[16] of the DPM, structure functions at an arbitrary scale of $q_\perp = 2$ GeV/c are employed for the excitaion function, but the essential difference between LUND and DPM remains in the use of the $1/\sqrt{x}$ distribution for the first excitation only.

Since for the $g(x) \propto 1/x$ both (43) and (45) give rise to the same $1/M$ string mass spectrum, it is sufficient to specify the string excitation algorithm in all three models referred to in (49) by (45). Thus, the interaction of two strings with initial light cone momenta, $E_1^{\pm}$ and $E_2^{\pm}$, with $E_1^+ > E_2^+$ and $E_1^- < E_2^-$, leads to two new

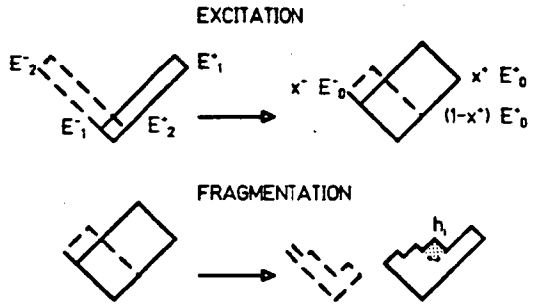

Figure 5: Illustration of an interaction of two strings with $E_1^{\pm}$ and $E_2^{\pm}$ in the Fritiof scheme[2] in momentum space followed by independent fragmentation into hadrons h_i.

strings with new momenta

$$\begin{aligned}(E_1^+, E_1^-, \vec{p}_{1\perp}) &\rightarrow (x^+E_0^+, (1-x^-)E_0^-, \vec{p}_{1\perp} + \vec{q}_\perp) \\ (E_2^+, E_2^-, \vec{p}_{2\perp}) &\rightarrow ((1-x^+)E_0^+, x^-E_0^-, \vec{p}_{2\perp} - \vec{q}_\perp) \ , \end{aligned} \tag{50}$$

according to the excitation law, $g(x^+, x_0^+)g(x^-, x_0^-)g_\perp(q_\perp)$, where $E_0^{\pm} = E_1^{\pm} + E_2^{\pm}$ and where the minimum momentum fractions are chosen to be $x_0^+ = E_2^+/E_0^+$ and $x_0^- = E_1^-/E_0^-$. The excitation of two interacting hadrons in the cm frame is illustrated in Fig. 5.

Finally, we note that the MCM parameterization in (49) with α left as a free parameter has been used in phenomenological analysis of pA data[18,19]. The value of $\alpha = 3$ has been found to reproduce a number of data. Of course, the reason that such diverse excitation functions as in (49) can be used to fit the data is that there is a great deal of freedom remaining in the specification of the fragmentation functions that describe how strings decay into the final hadrons.

An important conceptual difference arises between the LUND and DPM models when extended to p+A and A+A. In the LUND model it is assumed that multiple collision simple lead to further excitations of the same string with the same $1/x$ law. In DPM rescatterings involve the color exchange between different partons and thus lead to more and more strings. For a collision of a row of n nucleons on m nucleons, the LUND scheme leads to just $m + n$ highly excited string configurations, while DPM leads on the average to twice as many lower mass strings. In LUND all strings carry baryon number 1, but in DPM there are and equal number of generally lower mass $q\bar{q}$ strings. The number of possible string configurations possible to obtain in DPM by rewiring color flux lines between projectile and target nucleons is very large (see [16] for further details). This difference between LUND and DPM illustrate some of the basic theoretical uncertainties in the extrapolation from pp to AA even though both models tend to give similar results

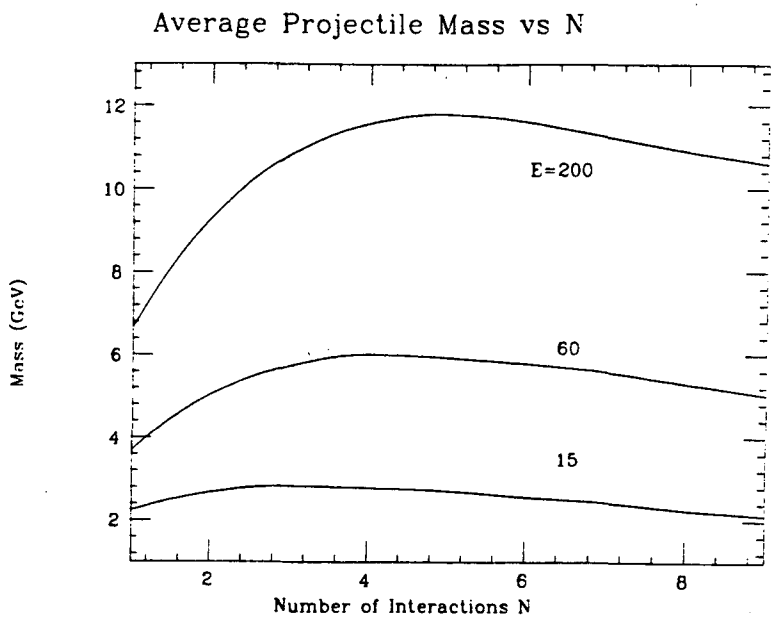

Figure 6: LUND string mass vs collision number at three incident energies

phenomenologically after an appropriate tune of parameters.

In Fig.6 the behavior of the invariant mass of an excited baryon string in the LUND model is shown as a function of the number of collisions it suffers in a nucleus. Note that the excitation mass increases to $\approx \sqrt{s}/2$ in all cases. For large N, the the mass eventually decreases due to energy loss (target string excitation). Note that string masses at the AGS are only ~ 2 GeV, so that finite energy effects can be expected to be important there.

2.2 String Fragmentation

Once the excited string configurations are determined, the second assumption is that those strings fragment independently as also illustrated in Fig.5. The seperation of the excitation and fragmentation phases is motivated by the long time scale expected for the fragmentation stage due to Lorentz time dilation as opposed to the short time scale of multiple interactions due to Lorentz contraction of the nuclei.

Given the light cone and transverse momenta of a string, its invariant mass and cm rapidity are given by

$$M^2 = E^+E^- - p_\perp^2 \ , \ Y = \tfrac{1}{2}\ln(E^+/E^-) \ . \tag{51}$$

High mass strings are of course unstable and break apart into low mass strings through $q\bar{q}$ pair production[10] The fragmentation of a string in momentum space

involves the subdivision of $E^{\pm}$ into pieces, $E_i^{\pm}$, such that $\sum_i E_i^{\pm} = E^{\pm}$. The light cone momentum fractions of the resulting hadrons are then

$$x_i^{\pm} = E_i^{\pm}/E^{\pm} \ .$$

The flavor composition and transverse momentum of the produced hadrons are determined by the flavors and transverse momenta of adjacent $q\bar{q}$ pairs that join to form the color singlet hadrons. If initially $\bar{q}_+$ carries the E^+ and q_- carries the E^- of the string and if N pairs $q_i\bar{q}_i$ with transverse momenta $\vec{p}_{\perp i}$ and $-\vec{p}_{\perp i}$ are produced from the $\bar{q}_+$ side to the q_- side. then the flavor composition and transverse momentum of the ith rank hadron are given by

$$\begin{aligned} h_i &= (q_i, \bar{q}_{i-1}) \\ \vec{k}_{\perp i} &= \vec{p}_{\perp i} - \vec{p}_{\perp(i-1)} \ , \end{aligned} \tag{52}$$

with $\bar{q}_0 = \bar{q}_+$ and $q_{N+1} = q_-$.

The dynamical quantity that controls the exclusive breakup probability, $\mathcal{P}_N(\{x_i^+, x_i^-, k_{\perp i}\})$, of the string is the fragmentation function, $f(x)$. In most fragmentation schemes the fragmentation of E^+ and E^- is assumed to proceed independently so that

$$\mathcal{P} \propto \prod_i f(u_i^+) f(u_i^-) \ , \tag{53}$$

where $u_i^{\pm}$ are *relative* momentum fractions

$$u_i^+ = x_i^+ / \left(1 - \sum_{j=1}^{i-1} x_j^+\right) \ , \ u_i^- = x_i^- / \left(\sum_{j=1}^{i} x_j^-\right) \ . \tag{54}$$

However, to join correctly the fragmentation from both ends it was shown in ref.[10] that the most general form of the fragmentation function that leads to left-right symmetry may also depend on the transverse mass of the produced hadron as

$$f(x, m_\perp) = \frac{(1-x)^a}{x} \exp(-b m_\perp^2 / x) \ , \tag{55}$$

where a and b are free parameters. The symmetric Lund fragmentation scheme thus leads to the following expression for the exclusive fragmentation probability:

$$\mathcal{P}_N(\{x_i^{\pm}, k_{\perp i}\}) \propto \prod_{i=1}^{N} p(q_i) f(u_i^+, m_{\perp i}) f_\perp(p_{\perp i}) \ , \tag{56}$$

where $m_{\perp i}^2 = x_i^+ x_i^- M^2$ is the transverse mass of the ith rank hadron and f has the special form (55). In (56), $f_\perp$ is the (Gaussian) transverse mometum distribution of produced quarks, and the $p(q_i)$ are *a priori* probabilities for producing flavors q_i.

In practice (56) is all that is needed to compute physical observables in momentum space. In particular, no space-time picture has to be assumed. However, there is a natural extension of string models that leads to an intuitive space-time picture of hadronization[10,51]. Adopting a completely classical picture of string dynamics, it is obvious that the string tension, $\kappa \sim 1$ GeV/fm, provides a conversion factor between momentum and coordinate spaces through the classical equations

$$dE^{\pm}/dz^{\pm} = \mp\kappa \quad , \quad dE^{\pm}/dz^{\mp} = 0 \ , \tag{57}$$

where $z^{\pm} = t \pm z$ are light cone coordinates.

With (57) we can translate string fragmentation into coordinate space. Consider again the fragmentation of an excited string ing of a diquark or antiquark with a large E^+ and negligible E^- and a quark with large E^- and negligible E^+. As the end points recede from each other along the light cones, they lose $E^{\pm}$ on account of (57) and turn around at at light cone coordinates $(z^+, z^-) = (L^+, 0)$ and $(0, L^-)$, where

$$L^{\pm} = E^{\pm}/\kappa$$

are the space-time lenght scales bounding the string fragmentation region. Suppose that the pairs $q_i\bar{q}_i$ are produced at light cone coordinates (z_i^+, z_i^-). Given the $E_i^{\pm}$ of the final hadrons, (57) constrains the production coordinates to be at

$$z_i^+ = L^+ - \sum_{j=1}^{i} E_j^+/\kappa \ , \ z_i^- = \sum_{j=1}^{i} E_i^-/\kappa \ . \tag{58}$$

Conversely, given the production coordinates, the transverse mass and rapidity of the ith rank hadron are given by

$$E_i^{\pm} = \kappa\Delta z_i^{\pm} \ , \ m_{\perp i}^2 = \kappa^2 \Delta z_i^+ \Delta z_i^- \ , \ y_i = \tfrac{1}{2}\log(\Delta z_i^+/\Delta z_i^-) \ , \tag{59}$$

where $\Delta z_i^+ = z_i^+ - z_{i+1}^+$ and $\Delta z_i^- = z_{i+1}^- - z_i^-$ as illustrated in fig.7

One of the advantages of considering string fragmentation in coordinate space is that the Schwinger formula for pair production in a constant field[45,46] provides a natural explanation for the form of the symmetric Lund fragmentation function (55). We briefly review the heuristic 'derivation' of (55) because it provides also a clue on how color rope fragmentation could occur. Note that the pair production points and classical trajectories define a polygon in space-time of area

$$A_{tz} = L^+\Delta z_1^- + (L^+ - \Delta z_1^+)\Delta z_2^- + \dots \ , \tag{60}$$

Inside the four volume

$$\Omega = A_{tz} A_{\perp} \ ,$$

where $A_{\perp}$ is the transverse area of the string, no pairs were produced by assumption. The probability that no pairs are produced in a four volume Ω can be estimated by Schwinger's vacuum persistence probability[45,46]

$$P_{\Omega} = \exp(-c\Omega\kappa^2) \ , \tag{61}$$

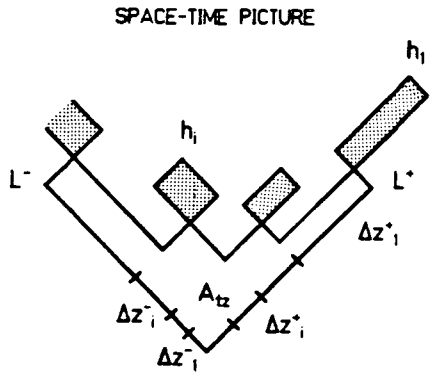

Figure 7: Fragmentation of a string via $q\bar{q}$ pair production followed by hadron formation in space-time.

where the constant c depends on the number of colors and flavors and whether self-screening is taken into account.

The probability for a single pair production event leading to a pair, each with a transverse mass, $m_\perp$, is given by the WKB tunneling formula[45]

$$P(m_\perp) = \exp(-\pi m_\perp^2/\kappa) \ , \tag{62}$$

This probability is independent of coordinate because a uniform field has been assumed. With (62), the probability of no pair production, (61), can be obtained from

$$P_\Omega = \prod_{\{q,p_\perp,x^\mu\in\Omega\}} (1 - P(m_\perp)) \ ,$$

as noted by Casher et. al.[45].

Combining, (61,62), the exclusive probability for string fragmentation can be obtained from

$$\mathcal{P}_N \propto \exp(-a\Omega\kappa^2)\prod_i \left\{\exp(-\pi(\mu_i^2 + p_{\perp i}^2)/\kappa)\right\} \ , \tag{63}$$

where μ_i and $\vec{p}_{\perp i}$ are the masses and transverse momenta of the produced quarks. To express Ω in terms of the transverse masses $m_{\perp i}$ and lightcone fractions $x_i^+ = E_i^+/E^+$ of the produced hadrons, we use (59) to rewrite (60) as

$$\begin{aligned} \kappa^2 A_{tz} &= E^+E_1^- + (E^+ - E_1^+)E_2^- + \cdots \\ &= E^+\frac{m_{\perp 1}^2}{x_1^+E^+} + E^+(1-x_1^+)\frac{m_{\perp 2}^2}{x_2^+E^+} + \cdots \\ &= \sum_i m_{\perp i}^2/u_i^+ \ , \end{aligned} \tag{64}$$

where u_i^+ are given by (54). With (64), we obtain finally

$$\mathcal{P}_N \propto \prod_i \left\{\exp(-\pi(\mu_i^2 + p_{\perp i}^2)/\kappa)\, f(u_i, m_{\perp i})\right\} \ , \tag{65}$$

where f is given by (55) with $a = 0$ and $b = cA_\perp$. In this way, we have derived a special case of the scaling fragmentation dynamics (56) from the Schwinger model. In this derivation the fragmentation parameter, a, was found to be zero. A plausible explanation of the physical origin of $a > 0$ needed phenomenologically to fit e^+e^- data may lie in finite size corrections[10].

With well chosen fragmentation parameters, the Lund scheme is able to reproduce the measured particle yields $\pi, K, \rho, K^*, \cdots$ including the hyperon yields in ~ 10 GeV strings produced in e^+e^-. This is important because high hyperon yields have been proposed as a signature of quark-gluon plasma formation. In order to determine quantitatively what constitutes "high", we need a model that reproduces the correct yields in manifestly non-equilibrium situations.

2.3 Color Ropes

The independence of multi-string fragmentation is certainly a strong model assumption, which may break down in heavy ion collisions if the string density is sufficiently large (see section 1.4). From Glauber geometry we expect a string density per unit transverse area $\rho_s \approx 2r_0\rho_0(A^{1/3} + B^{1/3})$ in *central* $A + B$ collisions. Thus, with $2r_0\rho_0 \approx 0.36$ fm^{-2}, ρ_s increases from $\sim 0.7/\text{fm}^2$ in pp to $\sim 2.5, 3.0, 4.3$ fm^2 in central pPb, OPb, and $PbPb$ collisions respectively. In this sense O^{16} beams lead to only a modest increase of ρ_s relative to p beams, while Pb beams should lead to about a factor of two enhancement of ρ_s. Fluctuations could increase locally those densities by another factor of two. (Note that the initial field energy density in this model is just $\epsilon \approx \kappa\rho_s$ with $\kappa \approx 1$ GeV/fm.) Nonlinear effects could manifest themselves if ρ_s exceeds some unknown critical value. We will consider one particular class of non-linear phenomena associated with possible color rope formation[47] to test the sensitivity of the results to uncertainties about the validity of the independent string hypothesis.

A Q-fold Abelian rope is defined as the superposition of Q parallel strings and any number of pairs of antiparallel strings such that the total electric charge at the end points is simply Q times larger than that in an elementary string. A random superposition of N strings leads on the average to $\langle Q \rangle = 0$ (i.e., a null rope) but fluctuations lead to an rms foldedness of $\langle Q^2 \rangle^{\frac{1}{2}} = \sqrt{N}$. In the non-Abelian case Q is a vector of the same dimension as the Cartan subspace (2 for SU(3)) with the important physical difference that gluon pair production contributes to its decay[46]. However, we consider here only a simplified treatment of Abelian ropes involving only $q\bar{q}$ decays.

Because the time scale for complete breaking of a rope is approximately independent of Q and occurs ~ 1 fm/c, there is no time for the transverse area of a rope to change appreciably during its decay and so we assume that it is a constant independent of Q as well. Since the fragmentation parameter, b, was found in (65) to depend only on $A_\perp$, and not on Q, the main effect of rope formation in this

model then is to modify the flavor suppression factors and transverse momentum distribution of the quarks in (65). For a Q-fold Abelian rope of area $A_\perp$, the electric field in the flux tube is $\mathcal{E} = Qg/A_\perp$, where g is the elementary charge. However, the effective rope tension entering the WKB formula (62) including final pair interactions is[45,46] $\kappa_Q = (Q - 1/2)g^2/A_\perp$, so that

$$\kappa_Q \sim 2Q\kappa_1 \ . \tag{66}$$

Combining (65,66), the ratio of flavor suppression factors should scale as

$$(q_j/q_i)_Q = \exp\left(\pi(\mu_i^2 - \mu_j^2)/\kappa_Q\right) \approx (q_j/q_i)_1^{\kappa_1/\kappa_Q} \ . \tag{67}$$

Furthermore, the Gaussian rms transverse momemtum parameter, σ_Q, should increase as

$$\sigma_Q = (\kappa_Q/\pi)^{\frac{1}{2}} \approx (\kappa_Q/\kappa_1)^{\frac{1}{2}}\sigma_1 \ . \tag{68}$$

In the LUND model the flavor suppression factors for elemetary strings are fitted to e^+e^- data to be

$$(d/u)_1 = 1 \ , \ (s/u)_1 = 0.3 \ , \ (qq/q)_1 = 0.1 \ , \ (c/u)_1 = 10^{-10} \ . \tag{69}$$

For a Q-fold rope, these suppression factors rapidly approach unity:

$$(s/u)_Q = e^{-1.2/Q} \ , \ (qq/q)_Q = e^{-2.3/Q} \ , \ (c/u) = e^{-23/Q} \ . \tag{70}$$

Consequently we expect higher abundances of strange hadrons, antibaryons, and even charmed hadrons could appear at rates comparable with hard processes if $Q \sim 5$ foldedness could be reached.

2.4 From pp to pA to AA

With this brief introduction to string models we turn to the problem of multiple collisions in nuclear collisions. The basic assumption here is that simple classical Glauber theory is sufficient to specify the probabilities for a multiple interactions between projectile and target nucleons. The basic LUND algorithm is readily translated into a Monte Carlo program. I have written my personal version called ATTILA[13] as a check of the nordic barbarian FRITIOF[10] and to explore the sensitivity of the results to variations of the many parameters and assumptions. A beautiful to fit to data should always be mistrusted. It is only useful to display a series of curves showing the variation of the results with reasonable variations of the rules. Conversely, a systematic deviation from data with increasing A may not mean evidence for QGP, but simply reflect part of the systematic uncertainty associated with a fixed set of assumptions extrapolated to novel conditions. For

example, it may be that the FRITIOF excitation algorithm is ok for the first three interactions and only starts to fails for subsequent ones because of some as yet unknown string dynamics effect implicite in models such as in section 1.4. With all these caveats, we must proceed cautiously.

The steps followed in a simple implementation of the LUND algorithm for nuclear collisions at a fixed impact parameter goes as follows: $\vec{b}$:

1. Initialize: Generate A_T target coordinates $\vec{x}_i$ and A_P projectile coordinates $\vec{x}'_i$ according to realistic Wood-Saxon densities. The projectile coordinates are shifted by $\vec{b}$. Generate rest frame Fermi momenta according to a Gaussian distribution of rms 0.25 GeV/c. Boost projectile and target strings to respective frames. Choose diquark-quark end point flavors according to SU(6).

2. Multiple Scatter: For each projectile nucleon, i, check all target nucleons,j, for an interaction as determined by

$$\begin{aligned} (x'_i - x_j)^2 + (y'_i - y_j)^2 &\leq \sigma_{in}/\pi \\ E'^{+}_i / E'^{-}_i &> E^{+}_j / E^{-}_j \quad , \end{aligned} \tag{71}$$

   where σ_{in} is the inelastic nn cross section taken as 32 mb. If (i,j) interact, then update light cone momenta, $E'^{\pm}_i$ and $E^{\pm}_j$ according to the chosen excitation law (49). A Gaussian random transverse momentum of rms 0.35 GeV/c is transferred between interacting strings.

3. Independent Fragmentation: Fragment all $A_T + A_P$ strings independently via a call to JETSET6.3 in the CERN program library. Filter exclusive event through experimental acceptances and store computed transverse energies, multiplicities, etc.

These steps are repeated typically 2000 times to accumulate statistics. Running time is approximately 1 hour for 2000 O+Pb events on a VAX8600.

To study the sensitivity of final results on the fragmentation parameters, calculations were performed with three different sets of fragmentation function parameters:

$$\begin{aligned} \text{Default(D} - \text{set)} : a &= 0.5, \ b = 0.9, \ \sigma_\perp = 0.35 \\ \text{Fiddled(F} - \text{set)} : a &= 1.0, \ b = 0.4, \ \sigma_\perp = 0.60 \\ \text{Rope(R} - \text{set)} : a &= 1.0, \ b = 0.4, \ \sigma = 1.2, \ Q = 4 \ . \end{aligned} \tag{72}$$

For the (4-fold) rope parameters, the flavor suppression factors were enhanced acording to (70) with Q=4. The parameter $\sigma_\perp$ is the rms width of the $p_\perp$ given to the produced $q\bar{q}$ pair. The motivation for the fiddled set is to reproduce the

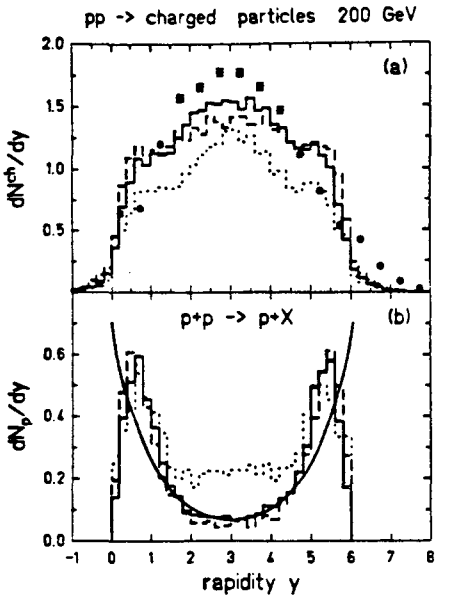

Figure 8: Charged particle and proton rapidity distributions and transverse moemntum distributions for 200 GeV pp computed via ATTILA with F-set (solid), D-set (long dashed), and R-set (short dashed) parameters. Data are from Demarzo et.al.

correct average transverse momentum of charged particles *without* having to introduce gluon kinks. The default set underestimates the average $p_\perp$ by about 20%. Fig.(8) compares the calculated rapidity densities with these parameters with pp data at 200 GeV. The transverse moemntum distributions are shown as well. We see that the effect of enhanced $p_\perp$ with the rope parameters leads to lower pion rapidity densities, but the enhanced anti-diquark production probability leads to higher baryon pair rate in the central region. In Fig.9 the dependence of the average transverse moemnta and baryon yields on the effective rope string tension are shown. Note that the pion transverse momenta are least sensitive to novel dynamics because they arise mostly from decays of heavy reonances. Particles such as K and p thus better reflect interesting new dynamics. Also note that the abundance hyperons and antihyperons increases very rapidly and saturates as a function of the effective string tension because the suppression of strange quarks goes away. What is clear from figs.8,9 is the strong correlation between different observables as we vary the assumptions and parameters of the string models. It is never enough to fit one observable such as the Σ^-/p ratio, but the correlation between all of the observables is the key to getting at the heart of the matter.

Turning to nuclear collision applications, Fig.10 compares p+U and Au+Au rapidity distributions from ATTILA and VENUS[16] versions of the string models. The important point to note is that while both models give approximately the same dN_{ch}/dy for $p+U$, the extrapolation to Au+Au differs dramatically. Remember that both models are simply extrapolating from the same pp and pA physics. In

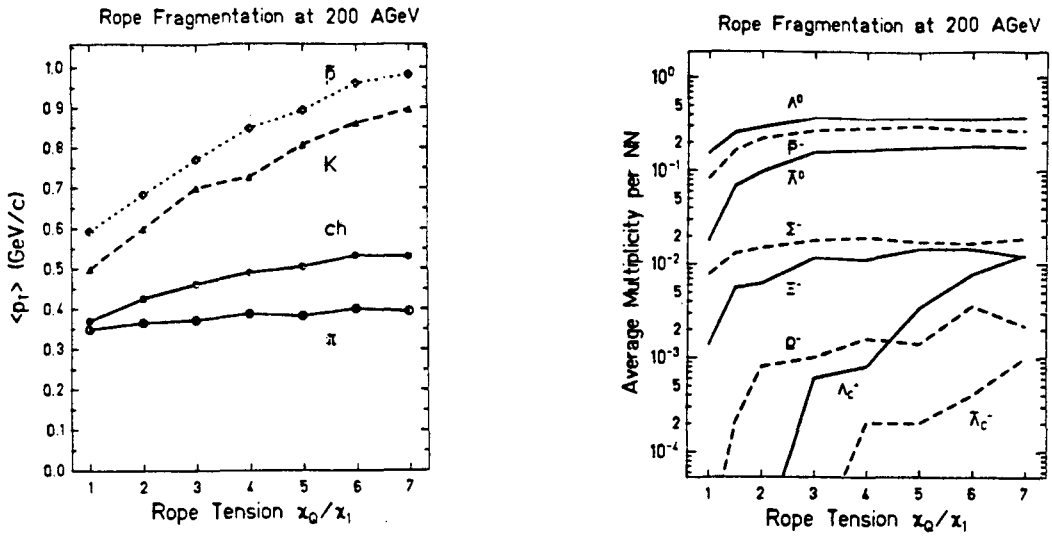

Figure 9: Effect of variations of the effective string tension in the schematic rope model on the transverse momenta and strange baryon yields

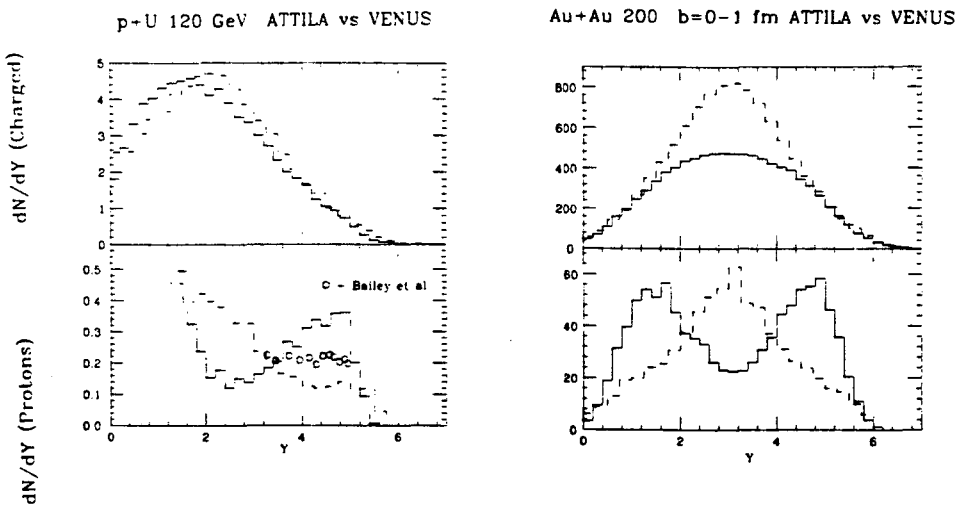

Figure 10: Charges particle and proton rapidity distribution from ATTILA (solid) and VENUS (dashed) models. Proton data is from Bailey et al

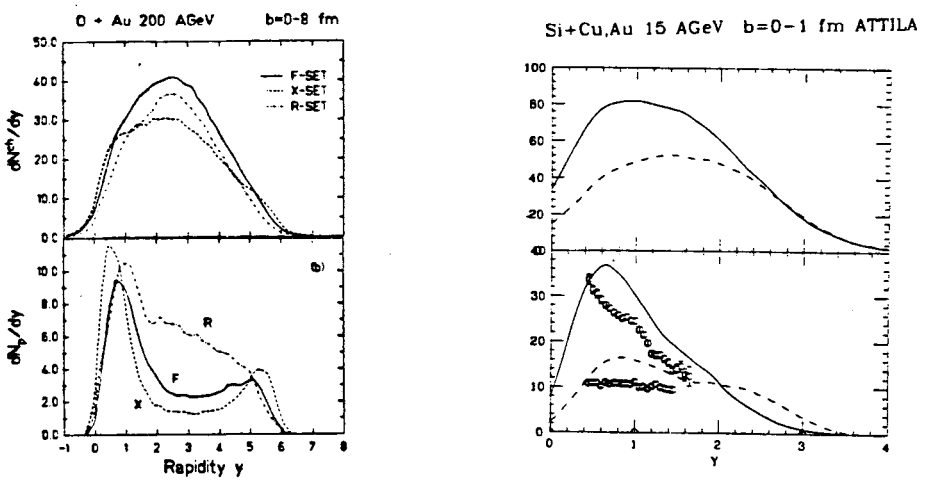

Figure 11: Sensitivity of rapidity densities to model assumptions. The AGS reactions were calculated using the F-set. The data are not final and used for illustration only.

fact comparison of the proton distributions with data[49] shows that there is a substantial difference in the mid rapidity region for protons where there is no data to compare with. In the limited domain where there is data neither model works so well. These uncertainties about pA dynamics for protons leads to a major uncertainty in Au+Au. The LUND model predicts a minimum for protons at $y \approx 3$ while VENUS predicts a strong maximum! The problem is that we still do not know enough about nuclear stopping power at high energies[50]. More precise measurements of p+A over a broader kinematical range is absolutely vital. It may be that Au+Au proton distributions will look more like VENUS predictions, however if p+U is found to be flat as expected from extrapolating the data, then the bump in Au+Au could be a signature of truly new and interesting phenomena.

In Fig.11 the sensitivity of the rapidity distributions to varying the LUND assumptions is illutrated. In addition the distributions for AGS energies is shown together with some extremely preliminary, non-quotable, raw data from E802 that is shown only for pedagogical purposes. (I thank Mr. Sarabaru of MIT for permission to show them). For O+Au at 200 AGeV we see that a rope mechanism (R-set) could significantly fill up the central region for protons but at the expense of pions due to the higher $p_\perp$ of the final particles. This then produces a differ-

ent correlation between proton densities and those other observables. The X-set curves involve the same fragmentation parameters as the F-set, but involve a restricted excitation mechanism of strings. The string masses are not allowed to increase beyond the value $\sim$ 6 GeV they reach in the *first* collision. The X-set curves thus test the effect of forbidding the increase of the string mass beyond the first interaction as assumed in the LUND algorithm. This is seen to lead to a major decrease in the inelasticity and a decrease of both pion and protons in the central region.

The curves for the central AGS reactions illustrate an important point. It is often assumed the AGS regime is one where the nuclear stopping power is large enough to create a central fireball. The LUND model shows however that while there is a large reduction of the projectile baryons around the beam rapidity, the target nucleons are only barely pushed pushed toward the central region. That is because the target nucleons are only hit only once or twice while the projectile nucleons are hit up to 6 times. Light nuclei are all surface and thus the ramp distribution found numerically is very reasonable. Is the ramp evidence for the formation of a high baryon density fireball? Since the LUND model can account well for, the answer would seem to be no. Based on the experience from the BEVALAC[23] only the heaviest mass nuclei are likely to form such a system.

3 Space-Time Aspects of Hadronization

3.1 Formation Zone in the Lund Model

In order to estimate the energy and baryon densities reached during nuclear collisions it is necessary to understand space-time development of hadronization. The LUND model generalized to coordinate space provides some insight into this problem assuming that momentum space is mapped linearly into coordinate space with an effective string tension κ, which may or may not coincide with the canonical 1 GeV/fm fitted from spectroscopy. The problem is illustrated in Fig.12 and we follow the discussion in refs.[51,52]. Consider the second rank hadron, which is formed by the quark q produced at P_1 and an antiquark $\bar{q}$, produced at P_2, and carries a fractional longitudinal momentum x. One possibility is to assume that it can rescatter beyond its "yoyo point", H_2, with $z = \ell_y(x)$, where the trajectories of q and $\bar{q}$ intersect for the first time. Another possibility is that its constituent antiquark $\bar{q}$ starts to interact with the nuclear medium immediately after it is created at P_2 with $z = \ell_c(x)$, which would correspond to a smaller effective formation length for that hadron. Subsequently, ℓ_y and ℓ_c will be referred to as yoyo length and constituent length, respectively. For a given x, one finds $\ell_y - \ell_c = xL$. Clearly, the difference between ℓ_y and ℓ_c and hence the ambiguity indefining the formation

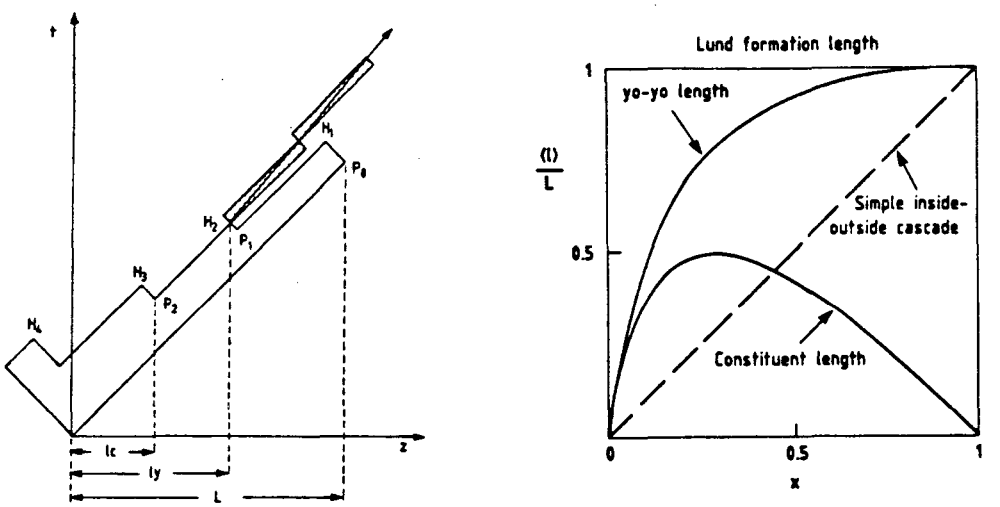

Figure 12: Space-time scales for hadronization. The difference between the constituent P_2 and the Yo-Yo H_2 points for the second rank hadron is illustrated. The average formation length of a hadron with fractional momentum x is also shown.

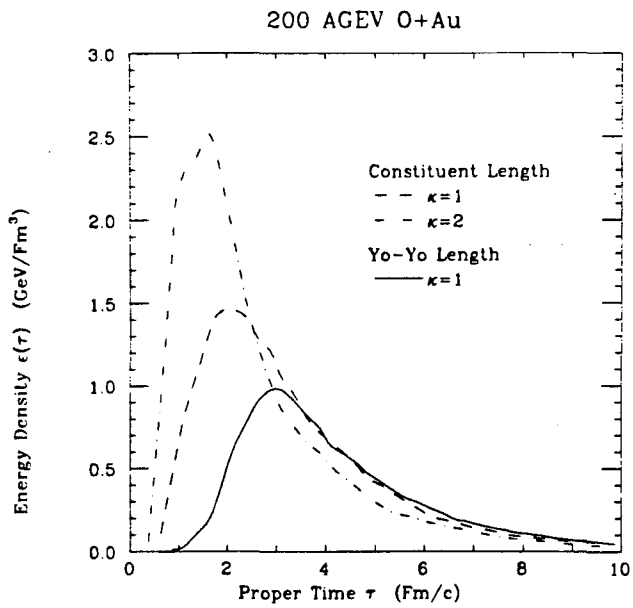

Figure 13: Sensitivity of the evolution of the central energy density to different assumptions about the formation length of secondary hadrons.

length are largest for $x \rightarrow 1$ as can also be seen from fig.12. The precise functional forms for the average formation length depends on the form of the fragmentation function. The curves shown are for a simple form, $(1-x^2)/x$, for illustration[51].

3.2 Evolution of the energy density

The basic ambiguity in defining the formation length of a composite particle must lead to an uncertainty about the values of the energy density achieved in nuclear collisions. Fig.13 shows the results obtained using ATTILA[13] for different assumptions. For O+Au at 200 AGeV the high density phase lasts at most 2 fm/c and energy densities achieved most of the reaction time involves energy densities below 1 GeV/Fm^3. Note however, that the maximum energy density reached is proportional to the effective string tension scale. This calculation includes the dilution effects of the finite nuclear geometries. This explains why the maximum energy density is a factor of 2-3 below the value the ideal Bjorken formula would give. Only at much higher energies, can the finite nuclear thickness be neglected.

What Fig.13 demonstrates that it is possible that the energy densities in present experiments fall considerably below the deconfinement scale. Therefore, a purely hadronic trasnsport theory may indeed be sufficient to explain many features of the

data. However, we emphasize the uncertainties in all estimates of energy density. We note that much higher energy densities were reported in ref.[16] using a variant of the DPM model[11]. In that case the high energy densities ~ 4 GeV/Fm^3 are due to the large number of very small mass $q\bar{q}$ pairs produced in that model, which are assumed to have zero formation time. At this stage we cannot even rule out the possibility that a Landau hydrdynamic shock wave with energy density $\epsilon_0 \sim 30$ GeV/Fm^3 is not created. All we can say is that if LUND type models can account for the observables, then the above calculation shows that the data are consistent with generating only a modest energy density, where plausably only hadronic degrees of fredom are important. In this sense a hadronic description of the dynamics of light ion reactions is self consistent.

3.3 Testing phase space dynamics in eA

In order to improve our understanding of the space-time development of hadronization it will be essential to study hadronization in e+A. The advantage of leptoproduction is that exactly one string is formed with fixed kinematics. A simple schematic model illustrates how e+A can help in this regard.

We are interested in A-dependence of particle production in the forward region in eA collisions. Consider a quark knocked out by a virtual photon along the z-axis at the point z_0. Let R denote the nuclear thickness. Suppose that a hadron produced in the quark fragmentation carries an energy fraction x. It will be formed at the point $z_0+\ell(x)$. The probabiltiy for that hadron to rescatter n times is simply

$$P_n(x_0, z_0) = \Theta(-z') \ \ \delta_{n0} + \ \Theta(z') \ \frac{1}{n!} \ (\frac{z'}{\lambda})^n \exp(-\frac{z'}{\lambda}) \ , \tag{73}$$

where $z' = R - z_0 - \ell(x_0)$ is the effective nuclear path traversed ny the hadron after its birth and $\lambda \equiv (\rho_0\sigma)^{-1}$ is the hadron's mean free path in the target nucleus, and σ the inelastic hadron-nucleon cross section. The dynamics is characterized by a scattering kernel $K_n(x, x_0)$, which is defined as the probability for a hadron of an initial energy fraction x_0 to be left with a fraction x after after being scattered n times on target nucleons.

The fragmentation function $D^{eA}(x)$ may then be written in a multiple collision expansion,

$$D^{eA}(x) \ = \ \sum_{n=0}^{\infty} D_n^{eA}(x) \tag{74}$$

where

$$D_n^{eA}(x) \ = \ \int_0^R \frac{dz_0}{R} \int_x^1 dx_0 \ D^{eN}(x_0) \ K_n(x, x_0) \ \ P_n(x_0, z_0) \tag{75}$$

The $n = 0$ contribution depends only on nuclear geometry,

$$D_0^{eA}(x) \ = \ D^{eN}(x) \ [\frac{\ell(x)}{R} + \frac{\lambda}{R}\{1 - \exp(-\frac{R - \ell(x)}{\lambda})\} \ ] \tag{76}$$

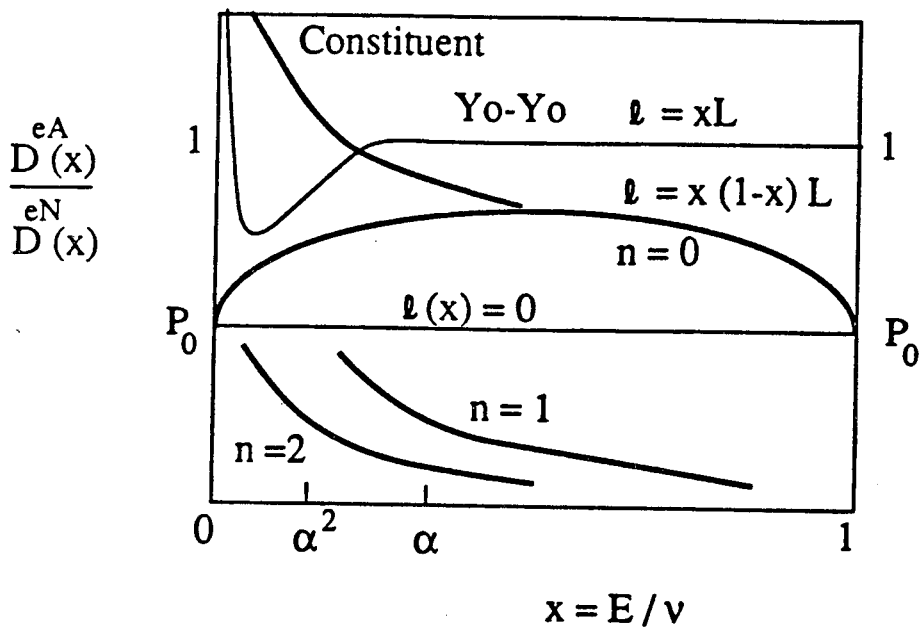

Figure 14: Sensitivity of fragmentation functions in eA to the formation length of secondary hadrons

The higher componenents are sensitive to the form of K_n. For illustration, consider the case of a fixed inelasticity $(1-\alpha)$ associated with every single collision, i.e. $K_n(x, x_0) = \delta(x - \alpha^n)$, which implies, for $n \geq 1$,

$$D_n^{eA}(x) \;=\; \frac{1}{\alpha^n}\, D^{eN}(\frac{x}{\alpha^n})\, \tilde{P}_n(\frac{x}{\alpha^n}) \tag{77}$$

where

$$\begin{aligned} \tilde{P}_n(x) \;&=\; \delta_{n0}\; [\Theta(\ell(x) - R) \;+\; \Theta(R - \ell(x))\, \frac{\ell(x)}{R}] \\ &+ \frac{\lambda}{R}\, [1 - \sum_{j=0}^{n} \frac{1}{j!}\, (\frac{R - \ell(x)}{\lambda})^j\; \exp(-\frac{R - \ell(x)}{\lambda})] \end{aligned} \tag{78}$$

The resulting ratio of fragmentation functions, $D^{eA}(x)/D^{eN}(x) = d\sigma^{eA}/dx/(Ad\sigma^{eN}/dx)$, is sketched in Fig.14, , where the simple parametrizations $\ell_y \sim xL$ and $\ell_c \sim x(1-x)L$ have been used for the yoyo and for the constituent formation length, respectively. The high x region can sort out the difference between yo-yo and constituent assumptions since the ratio at $x = 1$ is a pure Glauber factor $P_0(1)$. The low x region is sensitive to the rescattering of the produced particles which gives rise to second and third generation hadrons.

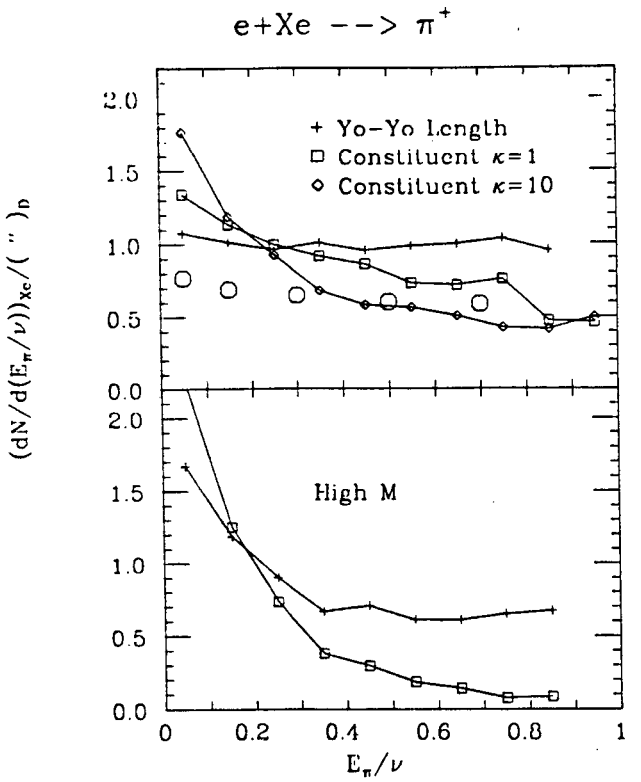

Figure 15: Calculated ratio of charged pion fragmentation functions for $e + Xe$ at 15 GeV. Data are from Osborne et al.

We have developed a complete LUND Monte Carlo program incorporating secondary cascading to test the above ideas in detail[52]. Unfortunately at present the data on low energy $\sim 10-30$ GeV eA of relevance for these studies is extremely sparse[53]. Figure 15 shows our preliminary findings for $e + Xe$ at 15 GeV for electron energy loss $\nu \sim 10$ GeV. The Yo-Yo length is clearly ruled out since it predicts too long formation lengths. The constituent length reproduces the high x region but fails to account for the substantial suppression of the pions at small x. The curve labeled $\kappa = 10$ corresponds essentially to a zero formation length hypothesis and nevertheless still fails to account for the suppression for $x < 0.2$. Further, zero formation length is ruled out since at $\nu \sim 100$ GeV the measured ratio goes to unity. We thus find that none of the formation zone models work in detail, assuming that the data[53] are correct. It is possible that there is a basic problem with the whole approach based on multiple scattering theory involving formation times. This would be very important to establish in this relatively clean case. An entirely different approach based for example an a dynamical Nambu string model[54] may be a more appropriate way to begin addressing this problem. The point is that any serious attempt to formulate a QGP transport theory for non-equilibrium phenomena should be tested on e+A and p+A first. It would be very useful if more data could be obtained in this energy domain.

3.4 Pion Interferometric Tests of Transport Models

Another approach to get a handle on the space-time aspects of hadronization is through pion interferometry (for a comprehensive review, see Zajc[55]). It is based on exploiting the constructive interference between identical bosons when their relative momenta are small compared to the inverse of the typical spatial dimensions of the reaction volume. Experimentally, the interference pattern is deduced by measuring like pion correlation functions,

$$C_n(\mathbf{k}_1, \cdots, \mathbf{k}_n) = \mathcal{N}_n P_n(\mathbf{k}_1, \cdots, \mathbf{k}_n) / \prod_{i=1}^{n} P_1(\mathbf{k}_i) \ , \tag{79}$$

where P_n denotes the n (identical) pion inclusive distributions, and $\mathcal{N}_n$ is the inverse of the normalized n^{th} factorial moment of the multiplicity distribution.

Present interest in this problem stems from new data on pion interferometry of nuclear collisions at CERN[56] that has been interpreted to provide possible evidence for QGP formation. The basic idea[57,58] is that if a QGP is formed, then the initial entropy density, σ_0, should be much higher than if the degrees of freedom were frozen into a hadronic gas. QCD lattice estimates (see Satz) indicate that there could be a large difference between the entropy density just below and just above the phase transition temperature, with $\sigma_0/\sigma_f \sim 3 - 10$. Since the total entropy of the system can only increase, the final decoupling volume of the system, V_f, must satisfy

$$V_f \geq (\sigma_0/\sigma_f) V_0 \sim (3 - 10) V_0 \ , \tag{80}$$

The initial volume is determined by the transverse area of the beam nucleus and the mean proper formation time of secondaries, which may be $\tau_0 \sim 1$ fm, i.e., $V_0 \approx \pi R^2 \tau_0 \approx 30$ fm^3. Therefore, we should look for a large change in the volume of the system. Pion interferometry is well suited for this task since the Bose interference pattern is only frozen in at the decoupling time, when the dimensions of the system exceed the pion mean free path.

Unfortunately, the problem is complicated by the strong correlations expected between momentum and space-time coordinates due to the inside-outside nature of hadron formation (see section 3.1). It is therefore essential to use of a more refined formalism[60,61] for the analysis of the data. The covariant current formalism[59,61] is suffiently general to address this problem leads to the following expression for the symmetrized m pion inclusive distribution:

$$P_m(k_1, \cdots, k_m) = \sum_{\sigma} \left\{ \prod_{i=1}^{m} G(k_i, k_{\sigma_i}) \right\} \ , \tag{81}$$

where $\sigma = (\sigma_1, \cdots, \sigma_m)$ runs over the $m!$ permutations of indices. The complex amplitude $G(k_i, k_j)$,

$$G(k_i, k_j) = \int d^4p D(k_i - k_j, p) j_0^*(pk_i/m) j_0(pk_j/m) \ , \tag{82}$$

involves the convolution of the Fourier transform of the "freeze-out" phase-space distribution

$$D(x,p) = \langle \delta^4(x - x_a)\delta^4(p - p_a)\rangle \ , \tag{83}$$

where $(x_a^\mu, p_a^\mu = mu_a^\mu)$ are pion freeze-out coordinates and momenta, with two current elements, j_0, that characterize the production dynamics. The current elements can also be thought of as the wavepackets of the outgoing pions[60].

In our calculations, we adopt a covariant pseudo-thermal model for the current elements which correspond to minimum Gaussian wavepackets in the pion rest frame[60]. This gives

$$j_0(pk/m) = \exp(-pk/(2mT)) \ . \tag{84}$$

where the effective "temperature", T, characterizes the spread of the source elements in momentum space and controls the transverse momentum distribution of the pions. With (84) the amplitude assumes the particularly simple form

$$G(k_1, k_2) = \langle \exp\{iqx_a - Kp_a/(mT)\}\rangle \ , \tag{85}$$

depending not only on $q^\mu = k_1^\mu - k_2^\mu$ but also on the mean pair momentum $K^\mu = \frac{1}{2}(k_1^\mu + k_2^\mu)$.

The effects of long lived resonances can be easily included in the semiclassical approximation. Note that the pion freeze-out coordinates, x_a^μ, are related to its parent resonance production coordinates, x_r^μ, through

$$x_a^\mu = x_r^\mu + u_r^\mu \tau \ , \tag{86}$$

where u_r^μ is the resonance four velocity and τ is the proper time of its decay. Inserting (86) into (85), summing over resonances r of widths Γ_r, and averaging over their decay proper times, we obtain the final expression

$$G(k_1, k_2) \approx \langle \sum_r f_r \, (1 - iqu_r/\Gamma_r)^{-1} \exp(iqx_r - Ku_r/T_r)\rangle \ , \tag{87}$$

where f_r is the fraction of the observed π^-'s arising from the decay of a resonance of type r, and T_r characterizes the decay distribution of that resonance. The factor $(1 - iqu_r/\Gamma_r)^{-1}$ insures that pions arising from decay of long lived resonances do not interfere effectively at moderate q.

The LUND model gives rise to a distribution of pions that can be characterized by a set of resonance fractions $\{f_r\}$, and a freeze-out phase space distribution of the form

$$D(x,p) \propto \tau e^{-\tau^2/\tau_f^2} e^{-(\eta - y)^2/2\Delta\eta^2} e^{-(y - y^*)^2/2Y_c^2} e^{-r_\perp^2/R_\perp^2} \ , \tag{88}$$

where τ_f specifies the width and mean value of the freeze-out proper time, $\tau = (t^2 - z^2)^{1/2}$, distribution, $\Delta\eta$ specifies the rms fluctuations of $\eta = \frac{1}{2}\log((t+z)/(t-z))$ around $y = \frac{1}{2}\log((E+p_z)/(E-p_z))$, Y_c is the width of the rapidity distribution

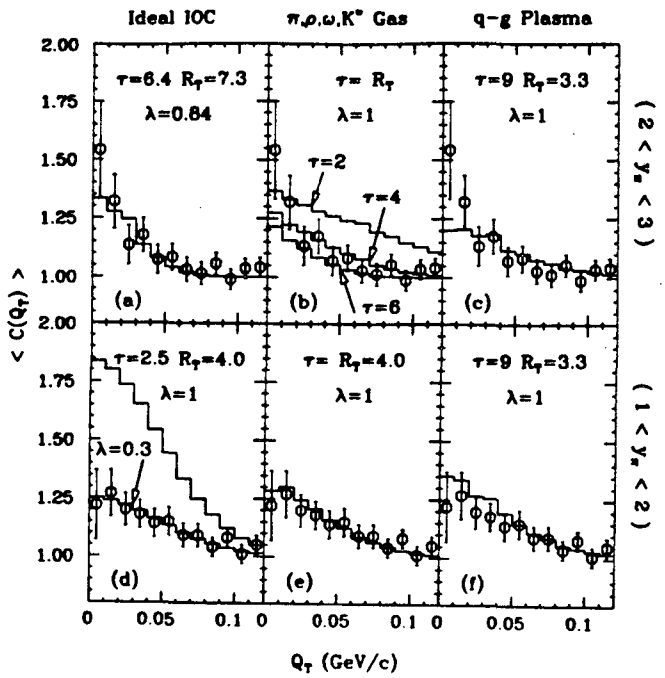

Figure 16: Analysis of the transverse projected $\pi^-\pi^-$ correlation data of NA35.

centered at y^*, and $R_\perp$ is the rms transverse radius at freeze-out. We have estimated the parameters of the freeze-out distribution and resonance fractions using the ATTILA version of the LUND, assuming a yoyo length formation zone and a string tension $\kappa = 1$ GeV/fm. For O+Au at 200 AGeV, we find that $Y_c \approx 1.4$, $y^* = 2.5$, $\Delta\eta \approx 0.7$, $\tau_f \approx 3$ fm/c and $R_\perp \approx 3$ fm. The π^- pedigree is determined to be $f_\pi = 0.19$, $f_\rho = 0.40$, $f_\omega = 0.16$, and $f_{K^*} = 0.09$, in rough agreement with data on hadron-hadron reactions. The contribution from longer lived resonances is set to zero.

In Ref.[58] a similar form for D was employed to parametrize the results of a quark-gluon plasma hydrodynamic calculation. In that case, the parameters were found to be $\tau_f = 9.0$ fm/c,$R_\perp = 3.3$ fm,$\Delta\eta = 0.76$, assuming that $Y_c = \infty$ and neglecting resonances. The characteristic long lifetime found in such hydrodynamic models is a direct consequence of an assume large latent heat of transition between the QGP and hadronic phases.

The results are shown in Fig. 16. For these calculations we chose $\Delta\eta = 0.8$ and considered $\tau_f = R_\perp = 2, 4, 6$ fm. We have performed an additional Monte Carlo hadronic cascade calculation taking as input the output of the ATTILA model and found that with a $\sigma = 20$ mb, the true freeze-out distribution is roughly characterized by $\tau_f \sim R_\perp \sim 4$ fm for this reaction. Parts a,b,c refer to pions in the central region and e,f,g to pions in the fragmentation regions. Parts a,d are the

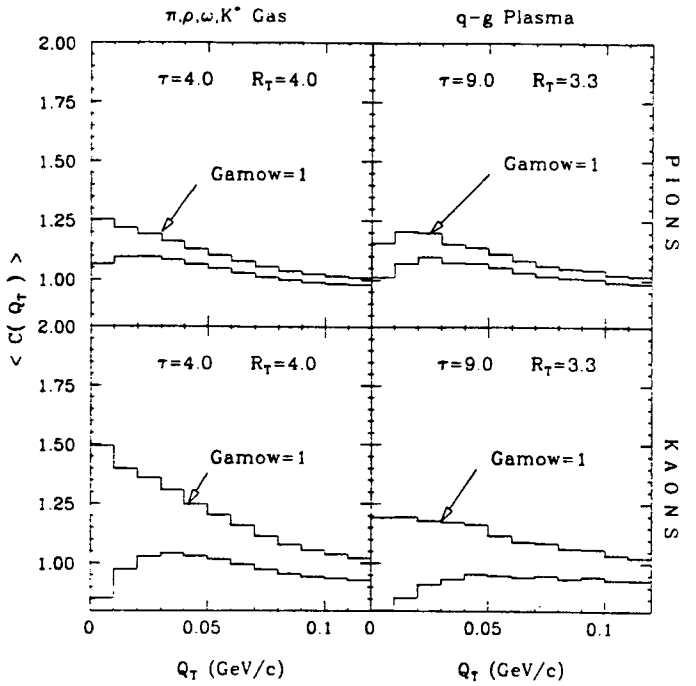

Figure 17: Kaon versus pion interferometry for O+Au at 200 AGeV.

fits found in NA35 using ideal inside-outside cascade parameterizations[59]. Our new results (b,e) and (c,f) correspond to completely chaotic sources.

It is clear that the present data are consistent with the freeze-out distribution expected on the basis of a resonance gas model for the nuclear dynamics. However, by numerical accident the data are also consistent with QGP freeze-out distribution[58]. The reason is that the long lifetime of the plasma source leads to the same effect in this case as the inclusion of long lived hadronic resonances, especially the ω.

To get around the accidental coincidence of the numerical results, we have recently computed the difference between kaon and pion interferometry[62]. Since kaons cannot arise from the decay of ω's, and the most important resonance source is the K^* with a much shorter lifetime, we can expect a much larger difference between the resonance gas and QGP predictions. In Fig.17 we compare the results. While the pion case is virtually identical in the two cases, there is a more pronounced difference in the kaon case because of the absence of the ω source. Unfortunately, the Coulomb Gamow correction is larger for kaons due to their higher mass, but with high enough statistics kaons could be a useful tool to probe differences between such extreme models. The premium will be on very high precision data.

Concluding Remarks

The premise of these lectures was that real progress in understanding high energy nuclear collisions will require the development of much more powerful transport models than known at present. There are fundamental theoretical problems open in every area of such work. Developing a transport theory incorporating the response of the QCD vacuumm condensates that are presumably responsible for confinement and chiral symmetry breaking is among the most important and fascinating challenges. Testing how far Nambu string dynamics could provide a transport theory in the confined phase is also of basic interest. Extending dynamical Abelian Higgs or Friedberg-Lee calculations to nuclear collisions could provide valuable hints into possible novel effects. Understanding why simple independent string models provide such a good description of at least light ion data is particularly important. It could be that in fact there are no dynamical strings in QCD at all and that the string models just accidently reproduce the same multiparticle distribution as more "conventional" QCD Bremsstrahlung type mechanisms[63]! In all models, we must face the problem of the proper space-time development of hadronization. In that connection I have emphasized that more detailed understanding of hadronization in eA would be particularly important. Maybe the A dependence of hard jet fragmentation could shed light on this problem. With the promise of a rich harvest of new data on pp, pA and AA collisions coming in the future, more work on such interesting dynamical issues is especially needed. On the long run, quark gluon plasma formation and diagnostics will become the central focus. However, as a prerequisite, the non-equilibrium aspects of ultra-relativistic nuclear collisions will have to be thoroughly understood.

Ackowledgements: I am very grateful to S. Gavin, M. Grabiak, M. Plümer, L. Robledo, and S. Padula for their valuable help in preparing these lectures.

References

[1] Proc. of 1st Workshop on Ultra-Relativistic Nuclear Collisions, May 1979, Berkeley, LBL-8957, UC-34C, CONF-7905107.

[2] H.Satz, ed., Statistical Mechanics of Quarks and Hadrons, Bielefeld Symposium 1980 (North Holland 1981).

[3] M. Jacob, H.Satz, eds., Quark Matter Formation and Heavy Ion Collisions,

Proc. of Bielefeld Workshop, May 1982 (World Scientific Pub. Co., Singapore, 1982).

[4] Proc. 3rd Intl. Conf. on Ultra Relativistic Nucleus Nucleus Collisions, eds. T.W.Ludlam, H.E.Wegner, Nucl.Phys. A418 (1984).

[5] K. Kajantie, ed., Quark Matter '84, Lecture Notes in Physics 221, (Springer-Verlag, Berlin, 1985)

[6] Quark Matter '86, eds. L.S. Schroeder, M. Gyulassy, Nucl. Phys. A461 (1987) 1c.

[7] Quark Matter '87, eds. H. satz, H.J.Specht, and R. Stock, Z. Physik C38 (1988) 1.

[8] Proc. Quark Matter '88, eds. G. Baym, P. Braun-Munzinger, S. Nagamiya, Nucl. Phys. A498 (1989) 1c-628c.

[9] E.V.Shuryak, Phys.Rep. 61C (1980) 71; The QCD Vacuum, Hadrons and the Superdense Matter, World Scientific Lecture Notes in Physics, Vol.8 (World Scientific, Singapore, 1988). D.J.Gross, R.D.Pisarski, L.G.Yaffe, Rev.Mod.Phys. 53; (1981) 43; B.Müller, The Physics of the Quark Gluon Plasmas, Lecture Notes in Physics 225, (Springer-Verlag, Berlin, 1985); M. Gyulassy, Prog. Part. Nucl. Phys. 15 (1985) 403.

[10] B. Andersson, et. al., Phys. Rep. 97 (1983) 31; Z. Phys. C20 (1983) 317; Nucl. Phys. B281 (1987) 289; Lund LU-TP-87-6 (1987);T. Sjostrand, JETSET manual, Lund preprints LU-TP-85-10, LU-TP-86-22.

[11] A. Capella, et. al. Z. Phys. C3 (1980) 68; C10 (1981) 249; C33 (1987) 541; Phys.Lett. 169B (1986) 285.

[12] V.Innocente, et. al., Phys.Lett. 169B (1986) 285.

[13] M. Gyulassy, CERN-TH.4794 (1987).

[14] P. Aurenche, F.B. Bopp, J. Ranft, Z. Phys. C23 (1984) 67.; H. J. Morhring, et. al. Z. Phys. C27 (1985) 419.

[15] J. Ranft, Phys. Lett. B188 (1987) 379.

[16] K. Werner, J. Hufner, M.Kutschera, O. Nachtmann, Phys. Rev. Lett. 57 (1986)1684; Phys. Lett. 183B (1987) 385; U. Heidelberg preprint HD-TVP-87-4 (1987).

[17] J.P. Pansart, Saclay preprint DPhPE 86-06 (1986); Nucl. Phys. A461 (1987) 521c.

[18] K. Kinoshita, A. Minaka, H. Sumiyoshi, Prog. Theor. Phys. 63 (1980) 928; S. Date, M. Gyulassy, H. Sumiyoshi, Phys. Rev. D32 (1985) 619.

[19] Y. Iga, R. Hamatsu, S. Yamazaki, H. Sumiyoshi, MGJC-HE-87-1 (1987) preprint (Matsusho Gakuen Junior College, Matsumoto, Japan); CERN-EP/87-53 (1987).

[20] T. Ludlam, BNL-preprints 51921 (1985), RHIC-PH-8 (1986).

[21] Proc. 2nd Heavy Ion Summer Study, LBL-3675, TID-4500-r62, UC-34c (1974).

[22] H. Stöcker and W. Greiner, Phys. Rep. 137 (1986) 277.

[23] S. Nagamiya, M. Gyulassy, Adv. Nucl. Phys. 13 (1984) 201.

[24] H. A. Gustafsson, et. al., Phys. Rev. Lett. 52 (1984) 1590; R. E. Renfordt, et. al., Phys. Rev. Lett. 53 (1984) 763;

[25] Proc. 8th Heavy Ion Study, LBL-24580, CONF-871116, UC-34C (1988).

[26] G. Peilert, et al, Phys. Rev. C39 (1989) 1402.

[27] G.F. Bertsch and S. Das Gupta, Phys. Rep. 160 (1988) 189.

[28] S. R. de Groot, W. A. van Leeuwen and Ch. G. van Weert: Relativistic Kinetic Theory, North-Holland, Amsterdam, 1980.

[29] J. Blocki, et al, Ann. Phys. 113 (1978) 330.

[30] P. Danielewicz, M. Gyulassy, Phys. Rev. D31 (1985) 53; A. Hosoya, K. Kajantie, Nucl. Phys. B250 (1985) 666; S. Gavin, Nucl. Phys. A435 (1985) 826.

[31] C. J. Pethic, G. Baym, H. Monien, Proc. Quark Matter 88 op.cit., in press

[32] M. Gyulassy, Nuclear Phase Transitions and Heavy Ion Reactions (eds, T.T.S. Kuo, D. Strottman, S.S. Wu, World Scientific, 1986) 83.

[33] U. Heinz, Phys. Rev. Lett 51 (1983) 351; Ann. Phys. 161 (1985) 48.

[34] H. T. Elze, M. Gyulassy, D. Vasak, Nucl. Phys. B276 (1986) 706; Phys. Lett. B177 (1986) 402; Ann. Phys. 73 (1987) 462.

[35] H.T. Elze and U. Heinz, CERN-TH.5325/89.

[36] S. Mrowsczynski, U. Regensburg preprint TPR-89-9 (1989).

[37] A. Bialas, W. Czyz, Z. Phys. C28 (1985) 255; Cracow preprint TPJU-8/89 (1989).

[38] J. Polonyi, Phys. Lett. B213 (1988) 340.

[39] R. A. Matzner, Computer in Physics, Sept. 1988, 51.

[40] H.B. Nielsen, P. Olsen, Nucl. Phys. B61 (1973) 45 G. 't Hooft, Physica Scripta 25 (1982) 133;

[41] J. W. Alcock, et al., Nucl. Phys. B226 (1983) 299.

[42] L. Robledo, private communication.

[43] T.D. Lee, Particle Physics and Introduction to Field Theory (Harwood Academic, New York ,1981).

[44] M. Bickeböller, et al, Phys. Rev. D31 (1985) 2892.

[45] A. Casher, et al.,Phys.Rev. D20 (1979) 179; N. K. Glendenning, M. Matsui, Phys. Rev. D28 (1983) 2890.

[46] M. Gyulassy, A. Iwazaki, Phys. Lett. 165B (1985) 157.

[47] T. S. Biro, H. B. Nielsen, J. Knoll, Nucl. Phys. B245 (1984) 449.

[48] C. De Marzo, et al, Phys. Rev. D26 (1982)1019.

[49] R. Bailey, et al, Z. Phys. C29 (1985) 1.

[50] W. Busza, R. Ledoux, Ann. Rev. Nucl. Part. Sci. (1988) 119.

[51] A. Bialas and M. Gyulassy, Nucl.Phys.B291 (1987) 793

[52] M. Gyulassy, M. Plümer, LBL-27605 (1989), Nucl. Phys. B in press.

[53] L.S. Osborne et al., Phys.Rev.Lett.40 (1978) 1624

[54] E. Remler, Proc. Int. Nuclear Workshop XVII, Hirschegg (1989); College of William and Mary preprint 1989.

[55] W. A. Zajc, Nevis Preprint R1384 (1987), to appear in Hadronic Multiparticle Production, World Scientific Press, P. Carruthers, ed. (1988).

[56] A. Bamberger, et al. (NA35 collab.) Phys. Lett. B203 (1988) 320.

[57] S. Pratt, Phys. Rev. D33 (1986) 1314.

[58] G. Bertsch, M. Gong, M. Tohyama, Phys. Rev. C37 (1988) 1896.

[59] K. Kolehmainen, M. Gyulassy, Phys. Lett. 180B (1986) 203;
M. Gyulassy, S. K. Kaufmann, and L. W. Wilson, Phys. Rev. C20 (1979) 2267.

[60] S. S. Padula, M. Gyulassy, S. Gavin, LBL-24674 (1989), Nucl. Phys. B, in press.

[61] M. Gyulassy, S.S. Padula, Phys. Lett. B217 (1988) 181.

[62] M. Gyulassy, S.S. Padula, LBL-27232 (1989), Phys. Rev. C in press.

[63] G. Marchesini and B. R. Weber, Nucl. Phys. B238 (1984) 1; J. F. Gunion and G. Bertsch, Phys. Rev. D25 (1982) 746; F. Niedermayer, Phys. Rev. D34 (1986) 3494.

LAWRENCE BERKELEY LABORATORY
TECHNICAL INFORMATION DEPARTMENT
1 CYCLOTRON ROAD
BERKELEY, CALIFORNIA 94720